Organic Geochemistry of the Cenomanian-Turonian Bahloul Formation Petroleum Source Rock, Central and Northern Tunisia

Hassene Affouri, Mabrouk Montacer, Jean-Robert Disnar

Organic Geochemistry of the Cenomanian–Turonian Bahloul Formation Petroleum Source Rock, Central and Northern Tunisia

H. Affouri [a*], M. Montacer [a] and J.-R. Disnar [b]

[a] Department of Earth Sciences, UR GEOGLOB (Code 03/UR/10-02), Faculty of Sciences of Sfax, University of Sfax, BP 1171, 3000 Sfax, Tunisia.

[b] ISTO (Institut des Sciences de la Terre d'Orléans), UMR 6113 CNRS/INSU - Université d'Orléans, 1A rue de la Férollerie, 45071 Orléans Cedex 2, France.

* Corresponding author: hassene.affouri@fss.rnu.tn; hassene_affouri@yahoo.fr.

Tel.: +216 98 65 67 02; Fax.: +216 74 27 44 37

ABSTRACT

Total organic carbon (TOC) determination, Rock-Eval pyrolysis, extractable organic matter content (EOM) fractionation, as well as gas chromatography (GC) and gas chromatography-mass spectrometry (GC-MS) analyses, were carried out on 79 samples from eleven outcrop cross sections of the Bahloul formation in central and northern Tunisia. The TOC content varied between 0.23 to 35.6%, the highest average values (18.73%, 8.46% and 4.02%) being at the east of the study area (at Ain Zakkar, Oued Bahloul and Dyr Ouled Yahia localities, respectively). The Rock-Eval maximum pyrolysis temperature (Tmax) values in the 424-453°C range delineated a general east-west trend increase in the organic matter (OM) maturity. The disparity in hydrogen index (HI) values, in the range 114-824 mg hydrocarbons (HC)/g TOC, is relevant for the discrepancy in the level of OM preservation and maturity among localities and samples.

The n-alkane distributions, maximizing in the C17 to C20 range, are typical for a marine planktonic origin, whereas pristine/phytane (Pr/Ph) average values in the 1-2 range indicate an oxic to suboxic depositional environment. Pr/n-C17 and Ph/n-C18 ratios in the 0.38-6.2 and 0.68-3.25 range, respectively, are consistent with other maturity indicators and the contribution of specific bacteria to phytol as a precursor of isoprenoids. The thermal maturity varies between the late diagenesis to the main-stage of petroleum generation based on the optic and the cis-trans isomerisation of the C29 sterane [20S/(20S+20R) and 14ß(H),17ß(H)/(14ß(H),17ß(H)+14α(H),17α(H)), respectively] and the terpane [18α(H)22,29,30-Trisnorneohopane/(18α(H)22,29,30-Trisnorneohopane+17α(H)22,29,30-Trisnorhopane): Ts/(Ts+Tm)] ratios. The Bahloul OM is represented by an open marine to estuarine algal facies with a specific bacterial contribution as revealed by the relative abundance of the ααα-20R C27 (33-44%), C28 (22-28%) and C29 (34-41%) steranes and by the total terpanes/total steranes ratio (1.2-5.33).

These results attested that the Bahloul OM richness was controlled both by an oxygen minimum zone induced by high productivity and restricted circulation in a narrow half graben structures and around diapirs of the Triassic salt.

Key words: Organic matter, Petroleum Source Rock, Cenomanian-Turonian, Bahloul Formation, biomarkers, steranes, terpanes, maturity, biodegradation, Tunisia.

1. INTRODUCTION

In central and northern Tunisia, the Cenomanian-Turonian (C/T) boundary succession is represented by thinly laminated carbonates with some marly beds assigned to the Bahloul Formation (Burollet, 1956). This formation was deposited during a so-called ocean anoxic event (OAE) (Schlanger et al., 1987a, b) or "E2 event" (Graciansky et al., 1982) and is interpreted to have been controlled by NE-SW, E-W and NW-SE trending horst and graben systems with syn-sedimentary normal faults (Layeb, 1990; Morgan et al., 1998; Soua et al., 2009). Reconstruction of depositional environments based on planktonic foraminifera suggests relatively deep-marine conditions, probably on the outer part of a horst and graben structured ramp and in a episodically confined environment (Caron et al., 2006; Zagrarni et al., 2008).

Previous investigations have shown that the organic matter (OM) in the Bahloul Formation is of marine planktonic origin and ranges from immature to mature in terms of hydrocarbon generation (Tissot and Welte, 1984; Affouri, 1996, 2004). In Tunisia, the Bahloul Formation is known to be a source rock for petroleum in Upper Cretaceous reservoirs, and also for its stratified sulphide (Pb-Zn)-hosted mineralization (Bishop, 1988; Montacer et al., 1988; Montacer, 1989, 1991; Layeb, 1990; Layeb and Belayouni, 1991, 2000; Yukler, 1994; Hughes and Reed, 1995; Bechtel et al., 1996, 1998). Seepage oils in northern Tunisia (in the diapir zone: Fig. 1) are interpreted to be, in part, derived from this formation (Belayouni et al., 1992; Gaaya and Ghanima, 1998).

The present study combines Rock-Eval pyrolysis and molecular geochemical data from eleven outcrop sections in central and northern Tunisia in order to evaluate the palaeogeographic and structural controls on the Bahloul Formation's deposition. Analysis of straight-chain alkanes, steranes and terpanes were used to investigate variations in the OM, and the heterogeneity of the OM which is related to palaeogeographic and structural controls

and to the nature of the water column. In addition, biological markers and Rock-Eval parameters were used to evaluate the origin, maturity and type of organic matter.

2. GEOLOGICAL SETTING

The Bahloul Formation is exposed at the surface over a wide area in central and northern Tunisia (Montacer, 1989; Layeb 1990; Montacer et al., 1995; Affouri, 1996, 2004) including the Tellian Atlas Zone (Tell. At.) and the Tunisian Atlas (Tn. At.) (Fig. 1). The Tellian Atlas is characterized by the stacking of allochthonous units (Rouvier, 1977) and a series of imbricate thrust slices (Zargouni, 1975; Perthuisot, 1978). The Tunisian Atlas zone includes the Northern Atlas, the central Atlas, the southernmost Atlas and the "North-South Axis". The northern Tunisian Atlas is characterized by the diapir zone (DZ) composed of numerous NE–SW-trending Triassic salt outcrops (Fig. 1) are in contact with younger Cretaceous and Cainozoic rocks (Perthuisot, 1978; Perthuisot, 1981; Burollet and Desforges, 1982; Boyer and Elliot, 1982; Snock et al., 1988). Local ascending movement of Triassic salt occurred during the Cretaceous (Orgeval, 1994; Patriat et al., 2003). The mechanism of the salt rising in this region is one of the most controversial subjects in the evolution of the northern Tunisian Atlas. Some authors explain the presence of the Triassic salt by a diapiric mechanism (Perthuisot, 1981), while others consider the Triassic salt outcrops to have been formed by large-scale allochtonous salt (glacier salt) movements interbedded within the Cretaceous layers (Vila et al., 1994; Vila et al.,, 1995). The central Atlas and the Northern Atlas are characterized by a bundle of NE-striking anticline folds that are cut orthogonally by a graben system. The southernmost Atlas is made up of E-W folds, inflected towards northeast at their terminations and bounded by the major northwest faults of Gafsa (Zargouni, 1985). To the east, the Tunisian Atlas is bounded by the North-South Axis (NOSA, Fig. 1: Burollet, 1956;

Anderson, 1991). The NOSA comprises a folded and faulted zone delimiting the central Atlas (sensu lato) and the Eastern Atlas. It corresponds to a major orogenic alignment with N-S trending faults (Burollet, 1956; Turki, 1985).

Subsidence during the C/T time led to the accumulation of a thick sequence (up to 80 m thick in Mellegue area, NW Tunisia (Fig. 1)) of laminated black shales and marls of the Bahloul Formation. Sharp variations in thickness and facies towards the north and northwest suggest that basin subsidence was driven by regional tectonic movements along NW-SE, NE-SW and E-W trending normal faults issued from Tethys and Sirte riftings. Formation of the Tunisian rift grabens was associated with the opening of the Neo-tethys to the north (Grasso et al., 1999) and the South and Equatorial Atlantic to the southwest (Maurin and Guiraud, 1993). Two Mesozoic rifting events occurred onshore Tunisia, namely (1) from the Late Jurassic to the Early Aptian, associated with E-W-trending half grabens and volcanism in the Pelagian sea, and (2) from the Late Aptian to Early Cenomanian, associated with NW–SE trending halfgrabens (Guiraud and Maurin, 1991). The two extensional events were interrupted by a regional Mid-Aptian uplifting phase which formed the unconformity shown in seismic data (Ibouh and Zargouni, 1998). Maximum thickness and peak organic-richness of the C/T strata are usually reached within the graben systems, most clearly documented in NW Tunisia. Rift movements had ceased (Grasso et al., 1999) or were subtle (Camoin, 1991) during deposition of the C/T deposits, and uplifting occurred only from the latest Cretaceous onwards (Soyer and Tricart, 1989; Grasso et al., 1999), hence, did not affect facies distribution of the C/T strata in Tunisia.

In parts of Tunisia, Cretaceous diapiric movements of Triassic salt also played a role in controlling C/T-deposition, e.g., in northern (Perthuisot, 1981) and central Tunisia (Bédir et al., 2001) and in the Pelagian Shelf (Camoin, 1991). Later, during the Upper Cretaceous, subsiding rim-synclines were created around the Triassic salt diapirs, thus, favouring the

installation of water stratification conditions and the high preserving sedimentation rates (Soua et al., 2009). In the vicinity of the diapirs, peridiapiric series is characterized by a marked thickness reduction, mainly in the marly members, and partly by development of a detrital facies (sandstones, conglomerates) (Perthuisot, 1981). The Albian to Middle Eocene diapiric rise was probably continuous, but it increased during periods of tectonic instability (Perthuisot, 1981; Grasso et al., 1999).

3. LITHOSTRATIGRAPHY

The Cenomanian-Turonian Bahloul Formation (Fig. 1) is composed of thinly laminated carbonates with some marly beds (Burollet, 1956) including euxinic facies with an oligospecific planktonic fauna (Ben Ferjani et al., 1990). Ammonites of the upper Cenomanian Actinocamax Plexus Zone have been recorded (Robaszynski et al., 1990) in the Kalaat Senan area. Microfauna are strictly planktonic (Ben Ferjani et al., 1990). At the Oued Bahloul type section (OBL, Fig. 1) (Burollet, 1956), a Cenomanian-Turonian age was proposed for the formation by Ben Hadj Ali et al. (1994). There have been many biostratigraphic, geochemical and sequence stratigraphic interpretations of the Bahloul Formation (Burollet, 1956; Robaszynski et al., 1993a, 1993b, 1993c; Ben Hadj Ali et al., 1994; Chaabani et al., 1994; Maamouri et al., 1994; Razgallah et al., 1994; Abdallah et al., 1995, 2000; Abdallah and Meister, 1997; Layeb et al., 2001; Luning et al., 2004; Caron et al., 2006; Soua and Tribovillard, 2007; Zagrarni et al., 2008). According to these studies, the majority of the formation in the study area was deposited as a transgressive systems tract (TST). Abdallah et al. (2000) dated the formation age as around the Cenomanian-Turonian boundary, in agreement with other authors; the lower part thus belongs to upper terminal

Cenomanian, and the overlying portion to the basal lower Turonian (Salaj, 1976; Montacer, 1989, 1991).

The planktonic foraminiferal fauna in the Bahloul Formation (Robaszynski et al., 1990) is composed of globular forms, dominated by the most primitive morphotypes that lived in the uppermost layer of the ocean (ca. 0–50 m). Their diversity is low but their productivity is high, characteristic of a colonizer fauna (Robaszynski et al., 1990). In black limestones of the Bahloul Formation, planktonic foraminifera are dominated by biserial forms (Heterohelix sp.), accompanied by globular trochospirales forms (Hedbergella sp. and Whiteinella sp., Caron et al., 1999). These foraminifera are thought to be opportunist species and to record fluctuations in nutrient supply: proliferation occurred during episodic increases in nutrient supply, but extinction took place as a result of modification of the environment (Caron et al., 1999). The biserial heterohelicids (Heterohelix spp.) are believed to be ecological opportunists and low-oxygen tolerant fauna thriving in well-stratified open marine settings with a well-developed oxygen minimum zone (OMZ). Thus, high abundance of Heterohelix indicates an expanded OMZ (Soua and Tribovillard, 2007). The triserial heterohelicacea Guembelitria species thrived in eutrophic surface waters with variable salinities at times of severe ecological stress (Soua and Tribovillard, 2007).

Radiolarians are common in Bahloul Formation. As reported by Caron et al. (1999), radiolarians and diatoms proliferated episodically associated with increased abundance of heterohelicids during deposition of the black laminated limestones of the Bahloul Formation. Radiolarian occurrences at the Oued Bahloul locality are interpreted as the first signals of episodic renewals of nutrient rich oceanic waters. Consequently, they could be used as indicators of an increase of water depth, and of better connections with open oceans. Heterohelix moremani and H. globulosa occur in high abundance together with numerous specimens of the genus Whiteinella (W. archaeocretacea and W. brittonensis) at Oued

Bahloul coinciding with the very first organic carbon-rich laminae. At this locality, the interval of high TOC values also records high $\delta^{13}C$ values. The correlation between TOC and $\delta^{13}C$ values observed at Oued Bahloul is indicative of good preservation of the primary organic matter in the section (Caron et al., 2006). In his study of depth profiles of selected geochemical tracers for the Bahloul Formation, Soua (2010; and references there in) concluded that the high values of V/(V + Ni), the high Cr/Al and the significant values of Mo/Al are indicative of oxygen depletion in bottom water-sediment interface during the deposition of the Bahloul Formation (Soua, 2010). Furthermore, this author noted that some levels from the Bahloul Formation showed slight enrichment in Barium (considered as a primary productivity proxy) that correlates with those of Cu and Ni. These observations associated with a positive excursion of the Ni/Al and Cu/Al ratios suggest an increased OM influx and also possibly records of increased primary productivity at the time of the Bahloul Formation deposition as confirmed by the abundance of radiolarian, at least at the Bargou locality (Soua, 2010).

At the Oued Bahloul locality, the "filaments" event occurs just above the C/T precision interval (Caron et al., 2006). Filaments, from their aspect in thin sections, were small bivalves that invaded oceanic nutrient rich environments, because of their short larval-planktonic phase (Jefferies and Milton, 1965). In a normal environment, they grew to their adult size; they progressively sank to the bottom where they survived in normal or moderate oxygenated environments. Caron et al. (2006) observed at the Oued Bahloul locality the downward migration led juveniles into O_2-deficient waters.

A palynofacies study showed that the OM in the Bahloul is dominated by amorphous marine algal or bacterial material (Caron et al., 1999). However, the occasional appearance of Botryococcus in marly limestones indicates a possible brackish-water or lagoonal depositional environment. Palynomorphs of terrestrial origin (pollen and spores) as well as phytoclasts

occur sporadically. These observations are consistent with a dysaerobic or anoxic depositional environments far from a continental source of material (Caron et al., 1999).

4. SAMPLES AND METHODS

Samples of the Bahloul Formation were recovered from eleven outcrops in central and northern Tunisia (Fig. 1). Sample sets were taken from surface outcrop sections located over a wide area in the central Atlas zone [Oued Bahloul, OBL; Ain Zakkar, AZ; Dyr Ouled Yahia, DOY (Bargou locality); and Kalaat Senan, SM] and in the Diapir Zone [from SW to NE, Garn El Halfaya, GH; Jebel Ksikiss, JK; Koudiat El Hamra, KEH; Koudiat Mghoutti Rassou, MR; Jebel Hadida, JH; Jebel Sabaa Koudiat, 7KT; and Oued Bazina, OBZ]. From the base to the top of each cross section, samples were selected regularly spaced (~ 1 to 2m) from unaltered black coloured, bituminous laminated marls and limestones levels.

Rock samples were powdered in an agate mortar. TOC determination was carried out using Rock-Eval pyrolysis under standard conditions with a Rock-Eval II apparatus equipped with a TOC module (Delsi Instruments; Espitalié et al., 1985). The Rock-Eval pyrolysis method consists of a programmed temperature heating (in a pyrolysis oven) under an inert atmosphere (helium) of a small sample (~100 mg) to quantitatively and selectively determine (1) the free hydrocarbons (S1) contained in the sample and (2) the potential hydrocarbons compounds (S2) that are volatilized during the cracking of the unextractable OM (kerogen) in the sample. The measured free hydrocarbons S1 value (mg hydrocarbons (HC)/g rock) represents those hydrocarbons pre-existing in the rock. The S2 values (mg HC/g rock) represent the remaining hydrocarbons generative capacity. The pyrolysis temperature Tmax (°C) is the temperature at which the S2 peak reaches its maximum. The Rock-Eval II apparatus can also be used to

determine the TOC of the sample by oxidizing (in an oxidation oven kept at 600°C) the organic matter remaining in the sample after pyrolysis (residual organic carbon). The TOC is then determined by adding the residual organic carbon detected to the pyrolyzed organic carbon, which in turn is measured from the hydrocarbon compounds issuing from pyrolysis.

The powdered samples were extracted with organic solvent ($CHCl_3$, 200 ml/30 g sample). The fraction which is recovered after solvent evaporation is called bitumen or extractable organic matter (EOM) (Durand, 1993; Hunt, 1995)**.** The bitumen was fractionated using liquid chromatography with a single column packed with activated silica gel, into saturate hydrocarbons (SHC), aromatic hydrocarbons (AHC) and polar compounds (NSO). The column was eluted with hexane to obtain the SHC and with hexane / $CHCl_3$ (65:35, v/v) to obtain the AHC. The NSOs were retained at the top of the column.

SHC were analysed using gas chromatography (GC) to investigate the distribution of linear and branched alkanes (n-alkanes and iso-alkanes, respectively), and gas chromatography-mass spectrometry (GC-MS) for cyclic alkanes (steranes and terpanes). GC was carried out using a Chrompack gas chromatograph (CP 9002) equipped with a flame ionization detector (FID) and a fused silica column (25m x 0.32 mm i.d.; CPSIL 5CB). The oven temperature programme was 120°C (1 min) to 290°C at 3°C/min, maintained at the latter temperature until elution of all compounds. N2 was the carrier gas.

GC-MS was performed with a HP 6890 series chromatograph equipped with a CPSIL 5 CB fused silica column (25m x 0.25mm i.d.) connected to a Hewlett Packard 5973 mass selective detector (MSD) by a 2 m capillary interface at 250°C. After splitless injection at 100°C for 1min, the oven temperature was increased to 310°C at 3°C/min. The MSD was operated using

the following conditions: 220°C; electron energy 70eV; scan range m/z 50-450; 1s per scan. He was the carrier gas. Peak height and relative intensities were measured from mass chromatograms of characteristic ions for steranes (m/z 217) and terpanes (m/z 191).

5. RESULTS

5.1. Bulk organic geochemistry

The Rock-Eval data (Table 1) show that TOC varied from 0.23 to 35.6%. The highest TOC contents (average values of 18.7%, 8.5% and 4.0%) occurred at the AZ, OBL and DOY localities, respectively, in the east of the study area. The JK samples contain a low TOC content (ca.0.6 % on average). The hydrogen index (HI=S2x100/TOC, mg HC/g TOC) corresponds to the peak S2 normalized for the TOC content and serves as indication of kerogen types (Tissot and Welte, 1984; Peters, 1986). Marine organisms and algae, in general, are composed of lipid- and protein-rich organic matter, where the ratio of H to C (H/C) is higher than in the carbohydrate-rich constituents of land plants. HI typically ranges from ~100 to 600 in geological samples. Here, HI values range from 114 to 824 mg HC/g TOC (Fig. 2), indicating that most samples contain Type II/III kerogen (Tissot et al., 1974). Tmax values between 424 and 453 °C indicate that the OM covers a range of maturities.

The extractable organic matter (EOM) ranges (Table 2) from 0.30 to 8.18 mg HC/g rock corresponding to ca. 1 to 20% of the TOC, making the formation a good to excellent petroleum source rock (Fig. 3) (Peters and Moldowan, 1993). The EOM content varies widely and one sample (JK4) had a value as high as 32% TOC. The NSO fraction generally

dominates the hydrocarbons (Table 2). Saturates dominate aromatics in all samples. At the Kalaat Senan locality, the SHC in SM samples represent ca. 14 to 74% of the EOM.

5.2. Biomarker composition

5.2.1. n-alkanes and iso-alkanes

Gas chromatography (GC) performed on the SHC fraction shows that the most of the samples have n-alkane distributions with a single mode maximizing in the C17 to C20 range and with a regular decrease towards higher carbon numbers (Fig. 4). The GH, KEH, OBL, DOY, AZ and OBZ samples are characterised by abundant steranes and terpanes in the C25 to C35 n-alkane range (Fig. 4). Two samples from the SM and JH sections (SM14 and JH5) show a bimodal distribution with maxima at n-C17/n-C18 and n-C24/n-C25 (Fig. 4).

Acyclic isoprenoids (iso-alcanes), especially pristane (Pr; i-C19) and phytane (Ph; i-C20) are relatively abundant in the SHC fraction. Pristane/phytane (Pr/Ph) ratios vary over a wide range of values (Table 2). The highest values (3.11; 3.09) occur in samples OBZ6 and OBZ8, respectively. The lowest values (<1) occur in samples SM10, KEH7 and OBZ3. All the other samples have Pr/Ph in the 1-2.84 range. Pr/n-C17 values (Table 2) vary from 0.38 to 6.2. The samples from the OBZ and AZ localities have the highest values, between 2.62 and 6.2 (Table 2). Ph/n-C18 values are very low and do not exceed 0.9 with the exception of the OBZ and AZ samples (0.68-3.25; Fig. 5).

5.2.2. Biomarkers: Hopanes and steranes

Eight samples were analysed for their terpane (m/z 191) and sterane (m/z 217) distributions (Fig. 6; Table 3). In all of them, terpanes (Fig. 6; Table 3) extend to C35 hopanes and are dominated by 17α(H), 21β(H) hopane αβC30H. The pattern of C31 to C35 homohopanes was C31 > C32 > C33 > C34 > C35 for samples OBL4, DOY4, GH2, SM14, JK2 and JH5; C31 > C32 ~ C33 > C34 > C35 for sample OBZ1; and C31 > C32 < C33 > C34 > C35 for sample OBZ5 (Fig. 6). Moretanes (i.e. 17β(H),21α(H)-moretanes βαC29 and βαC30) are relatively abundant in samples OBL4, GH2, DOY4, OBZ1 and OBZ5 (Fig. 6). The m/z 191 chromatograms for samples JK2 and SM14 (Fig. 6) are characterised by significant extended tricyclic terpanes from C20 to C29 (Ekweozor and Strausz, 1982), high 18α(H)-trisnorneohopane (Ts) versus 17α(H)-trisnorhopane (Tm), and a very low concentration of the C29 and C30 moretanes. Gammacerane is present in low concentrations in most of the samples.

The sterane (m/z 217) fingerprints are displayed in Fig. 6. All eight samples contain C27 to C30 steranes (Fig. 6; Table 3). Low amounts of C30 steranes, much lower than those of the C27 to C29 steranes, occur in samples DOY4, GH2 and OBZ1. All the other samples contain very low amounts of C30 steranes or even zero. The proportions of diasteranes are low compared to regular steranes with the exception of sample JK2 (Fig. 6). Sample JH5 shows a poor m/z 217 chromatogram (Fig. 6). All samples contain only small amounts of the 14α(H),17β(H)-20R C28 sterane (αα20R C28) relative to the C27 and C29 homologues. The proportion of 14α(H),17β(H)-20R C27 (αα20R C27) varies irregularly among the samples. The distribution patterns are αα20R C29 sterane > αα20R C27 sterane for samples OBL4, GH2, SM14, JH5, OBZ1 and OBZ5; and the reverse (i.e. αα20R C27 > αα20R C29) for samples DOY4 and JK2 (Fig. 6; Table 3). The OBL4, DOY4, GH2, OBZ1 and OBZ5 sterane

distributions are dominated by the biogenic configuration, i.e. αα20R C27, C28 and C29 regular steranes (Fig. 6; Table 3). By contrast, the 14β(H),17β(H)-20R (ββ20R) and 14β(H),17β(H)-20S (ββ20S) isomers dominate over the αα20R and 20S compounds in samples SM14, JK2 and JH5.

6. DISCUSSION

6.1. Source rock OM richness and typing

It is known that adequate amount of OM is a necessary requirement for rock to generate oil or gas (Cornford, 1986). TOC is a measure of the OM richness of a rock, i.e. it is the quantity of organic carbon (both kerogen and bitumen) in a rock sample (Jarvie, 1991; Peters and Casa, 1994). The TOC content varies widely between samples and localities (Table 1), with two general patterns: (i) the highest TOC contents occurred at the OBL, DOY and AZ localities in the east of the study area; and (ii) at each location, TOC concentration was in general higher at the base of the formation and decreases up-section.

The lateral variations suggest differences in palaeo-depositional setting between the localities, resulting in the decreasing TOC trend from E to W (Fig. 7). TOC concentrations on the seafloor may record variations in surface bioproductivity and/or OM preservation during sedimentation and early diagenesis. The Bahloul Formation was deposited in a basin which was controlled by local vertical Triassic salt movement (Orgeval, 1994; Patriat et al., 2003) and by half graben rifting (Abdallah and Meister, 1997; Grasso et al., 1999; Morgan et al., 1998; Soua and Tribovillard, 2007; Soua et al., 2009). Thus, the highest TOC contents coincide with peri-diapiric Triassic salt diapirs and grabens zone. In these settings, high

surface productivity induced by upwelling was responsible for the development of an oxygen minimum zone (OMZ) in the intermediate water column as suggested by Lüning et al., (2004) who interpreted the increased rate (70%) of small Heterohelix (H. Moreman, succeeded H. pulchra, H. navarroensis) that are considered residents of low dissolved oxygen marine waters, as indicative of the installation of the OMZ. Furthermore, in the deepest parts of the narrow half-graben structures particularly at the Oued Bahloul, Ain Zakkar and Dyr Ouled Yahia localities belonging to the Jebel Serdj and Bargou palaeohigh (Soua et al., 2009), caused restricted circulation to occur which favoured OM preservation. High HI average values (298 mg HC/g TOC< HI< 696 mg HC/ g TOC; Fig. 8b) at the OBL, AZ, DOY, 7KT, KEH-MR, GH and OBZ localities are consistent with well-preserved, immature to marginally mature Type II OM deposited in an anoxic to sub-oxic environment (Fig. 8b). By contrast, low HI average values (HI< 300 mg HC/ g TOC) at the SM, JK and JH localities are consistent with a more advanced stage of maturation (Fig. 8b).

6.2. Thermal maturity

Thermal maturity describes the extend of heat-driven reactions which convert sedimentary OM into petroleum (Peters and Moldowan, 1993). OM can be described as thermally immature (diagenesis stage), mature (catagenesis stage) or post-mature (metagenesis stage) depending on its relation to the oil-generative window (Tissot and Welte, 1984). Since the conversion of kerogen to bitumen during hydrocarbon generation with increasing thermal stress due to burial, the S2 peak decreases and S1 increases. The ratio S1/ (S1+S2), called the production index [PI, (%)] should increase with increasing maturity. PI values of 0 to 10% are taken as indicative of immaturity. Values from 10% to 40% characterize the interval from the onset to peak oil generation, while higher values are indicative of contamination from

migrated oil. The Tmax is frequently used as a maturity indicator, because as maturity of a kerogen increases, the temperature at which occurs the maximum rate of pyrolysis increases. According to Espitalie et al. (1985) the oil window (catagenesis stage) is defined by the following Tmax ranges: 440ºC-448ºC for Type I OM, 430ºC-455ºC for Type II OM and 430º-470ºC type Type III OM. Rock-Eval results are often plotted on a cross-plot of HI versus Tmax to constrain OM type and maturity (Fig. 2). The PI was used to indicate the presence of migrated oil and as an additional maturity parameter (Table 1).

Tmax values of 424-453°C indicate that the samples cover a wide range of maturities. Values do not vary significantly within each section, but there is a general east-to-west trend of increasing maturity (Fig. 8a). As indicated by Tmax values of about 425°C, the Ain Zakkar samples (AZ) contain thermally immature OM (at the end-diagenesis stage) with respect to petroleum generation (Espitalié et al, 1977; Peters, 1986). The OBL, DOY, GH, KEH, MR and OBZ samples (Fig. 8a), with Tmax of 429-440°C (Espitalié et al., 1985) have reached the onset of oil generation. The higher maturity of the SM, JK, and JH samples indicated by Tmax values of 439-453°C is consistent with greater burial of the OM and/or the higher geothermal gradient in these areas (Ben Dhia, 1987). A plot of HI versus Tmax (Fig. 2) indicates that, despite the observed variations in maturity, the Bahloul Formation has preserved a typical Type II OM signature. The diagram also shows that the east-to-west decrease in HI values is accompanied by an increase of Tmax values.

The EOM in petroleum source rocks consists of a highly complex mixture of molecules, covering a wide range of structural types, molecular weights and functionalities. A biological marker or biomarker (Eglinton and Calvin, 1967) which could be any organic molecule found in geological samples is used to identify such compounds. These biomarkers are organic molecules derived from formally living organisms through biological processes which show pronounced resistance to chemical changes. Any alteration of the original biological chemical

during burial and maturation should be minimal thereby keeping the fundamental carbon skeleton intact. The functional groups (-OH, =O etc.) may be lost but the biological origins may still be recognised (Briggs, 2007).

The SHC typically used as biomarkers include steranes, terpanes and the isoprenoids pristane and phytane (Seifert and Moldowan, 1981). For the purpose of this study, the emphasis will be on the acyclic isoprenoids, hopanes and steranes. The ratios of isoprenoids to n-alkanes are widely used since they provide informations on maturation and biodegradation as well as source (Ficken et al., 2002; Roushdi et al., 2010). The isoprenoids/n-alkanes [Pr/n-C17 and Ph/n-C18] ratios indicate the source rock facies and maturity (Hunt, 1995). The values decrease with maturation as a result of thermal cracking that produces n-alkanes and progressively eliminates Pr and Ph (Tissot et al., 1971). Both Pr/n-C17 and Ph/n-C18 ratios increase progressively with n-alkane biodegradation (Peters et al., 1999).

In our samples, the relatively high yield of bitumen per gram TOC for mature and even immature or marginally-mature samples (1.7-32.6%), thermal generation of bitumen occurred locally. The low PI values (Table 1) suggest the EOM is indigenous and has not migrated from elsewhere. Fig. 5 indicates wide variations among the samples. The low Pr/n-C17 and Pr/n-C18 ratios (<1) indicate that the SM, JK and JH samples fit into the maturity boundary of the cross plot with respect to thermal maturity. By contrast, high Pr/n-C17 and Pr/n-C18 ratio values, that suggest immature to marginally mature samples, are consistent with biodegraded n-alkanes. This is especially the case for samples OBZ, DOY and AZ which belong to the biodegradation side of the diagram (Fig. 5).

Hopanes are ubiquitous in petroleum source rocks and crude oils. These compounds are thought to be derived mainly from a specific oxygenated precursors (such as bacteriohopanetetrol), found in the cell walls of prokaryotic organisms (Requejo and Halpern, 1989), and commonly occur as a homologous series of structurally related isomers containing

between 27 and 35 carbon atoms. The stereochemical configuration of hopanes changes irreversibly with thermal stress from their biological configuration 17β(H), 21β(H) (ββ) to a both βα (moretane) and αβ (hopane) configuration (Seifert and Moldowan, 1980).

The 17α(H), 21β(H) homohopane isomerization ratios (%SC31; Table 4), tending to a value of 57% (Fig. 8c), indicate that most of the samples have attained thermal equilibrium (Seifert and Moldowan, 1986). However, sample SM14 exhibits a low value (45%, Table 4) which is not consistent with its advanced maturity as indicated by other criteria (Table 1, Figs. 4 and 6). The low value for this sample could be due to primary migration of generated oil. For this sample, this interpretation is consistent with the high PI and EOM/TOC values of 15% and 8%, respectively (Tables 1 and 2). Alternatively, the broad nature of the C31 R compound, for this SM14 sample, could indicate coelution with a contaminant. In the other hand, the 17α(H), 21β(H) bishomohopane isomerization ratios (%SC32; Table 4) are generally consistent with the Tmax. values with exception of the samples OBL4 and DOY4. These latter should have attained equilibrium values of this ratio at the early stage or at the end of the diagenesis.

The moretane/hopane ratio (30M/30H, Table 4) decreases with increasing maturity from values of about 0.8 for immature bitumen to less than 0.15 for mature samples, and finally to a minimum value of 0.05 (Grantham, 1986a). Values are in the 0.16-0.24 range for the immature to marginally mature samples OBL4, DOY4 OBZ1, OBZ5 and GH5 (Table 4), the lowest value (0.14) representing the mature sample JH5. Moretanes are absent or present in very low concentrations for samples SM14 and JK2 (Fig. 6; Table 4). The values are in agreement with the maturities as deduced from the Rock-Eval data at these localities (Table 1 and Fig. 2).

The Ts/Ts+Tm ratio (%Ts, Table 4) depends on both source and maturity (Moldowan et al., 1986). Ts is thermodynamically more stable than Tm (Peters and Moldowan, 1993), and the ratio therefore increases with increasing maturity. Samples SM14, JK2 and JH5 have ratio values of 66%, 73% and 55%, respectively (Table 4), consistent with thermally mature OM (Fig. 8d). Values in the range 16-40% for samples OBL4, DOY4, GH5, OBZ1 and OBZ5 indicate immature to marginally mature OM at these localities. The hopane maturity indices are consistent with the Rock-Eval results and the GC results for saturate hydrocarbons, indicating a general east-west trend of increasing maturity (Fig. 8d).

The tricyclic terpane (C23T to C28T, Table 3) distribution varies significantly and irregularly. Tricylic terpanes are generated from kerogen at a relatively high degree of maturity (Peters et al., 1990), C23T being usually prominent (Connan et al., 1980; Sierra et al., 1984). The C23T to C30 hopane ratio (23T/30H, Table 4) has been used as a maturity parameter (Peters et al., 1990). Ourisson et al. (1982) proposed that tricyclohexaprenol from prokaryote membranes is a precursor of tricyclic terpanes containing <30 carbons. Tricyclic terpanes have also been associated with the alga Tasmanites (Revill et al., 1994). Kruge et al. (1990) attributed abundant tricyclic terpanes to a common feature of a freshwater environment. In contrast, de Grande et al. (1993) reported prominent tricyclic terpanes for saline lacustrine and marine carbonate environments. Dahl et al. (1993) suggested that C23T/C30H values could be inversely related to anoxia and/or salinity, the rationale being that hopane precursors predominate in conditions of pronounced anoxia and/or salinity whereas the abundance of tricyclic terpane precursors increases under more oxic and/or less saline conditions (Bennett and Olsen, 2007). Samples OBL4, DOY4, SM14, JK2 and GH2 contain significant amounts of tricyclic terpanes (C21T-C28T), C23T being the most abundant. The 23T/30H ratio values in the 0.06 to 0.26 range (Table 4) are consistent with %Ts values. Sample SM14 has the

highest value (0.26), suggesting thermal generation of these compounds. By contrast, the mature samples JK2 and JH5 contain very small or no significant amounts of tricyclic terpanes, respectively. The absence of tricyclics in these two samples could indicate a proximal clastic facies. These samples have the lowest 29H/30H hopane ratio (Table 4).

As for hopanes, the initial C-20R configuration of 14α(H),17α(H) steranes is progressively converted to 20S with increasing thermal stress (Seifert and Moldowan, 1986), a value of ca. 40% corresponding to the beginning of oil generation (Mackenzie et al., 1980). Here, the [20S/(20S+20R)]-14α(H),17α(H) C29 regular sterane ratio values (%ααS) ranges from 23% to 45% (Table 5; Fig. 9), the highest value being displayed by sample OBL4 (Fig. 10a). This high value is inconsistent with the thermal immaturity of this sample as indicated by Rock-Eval maturity parameters (Table 1), EOM/TOC ratio (1.7%; Table 2) and %Ts (30%; Table 4). Furthermore, these parameters also being consistent with an absence of oil staining. Thus, the high sterane isomerization value of sample OBL4 might result from incipient bacterial degradation of the 20R steranes (e.g. Seifert et al., 1984). However, sterane biodegradation is normally not expected before the complete removal of n-alkanes and isoprenoids (Connan, 1984; Tissot and Welte, 1984), but the alkane distribution of sample OBL4 appears to be intact (Fig. 4). Thus, for this sample, sterane biodegradation may have preceded n-alkane generation during burial (Hu Ming-An et al., 1995). For the other samples, the %ααS sterane ratio is consistent with %Ts values. This result corroborates the fact that the isomerization of these biomarkers is due to the effect of increasing thermal stress, sterane isomerization having not reached the equilibrium value of ca. 52-55 % (Seifert and Moldowan, 1986).

The ββ20R/(ββ20R+αα20R) C29 sterane (%ββR) values for samples SM14, JK2 and DOY4 are 52, 56 and 34 %, respectively (Table 5), lower than the equilibrium value of 67-71%

(Seifert and Moldowan, 1986). The values are consistent with the thermal immaturity of sample DOY, and the more advanced maturity reached at SM and JK localities. The values also agree with other biomarker maturity parameters, namely the %Ts and the %ααS.

The abundance of diasteranes reflects both the effect of the mineral matrix and maturity. The 20S/20S+20R C27 diasterane (%SDia) ratio has reached values of ca. 62% for samples OBZ1, OBZ5, DOY4 and GH2, and 66% and 65% for samples SM14 and JK2, respectively (Table 5). Sample OBL4 displays the highest value (74%) (Table 5). Except for this sample, the %SDia ratio values correlate well with those of %Ts. This correlation is consistent with a thermal origin of these diasteranes. The high diasterane content of the thermally immature sample OBL4 may be due to the high clay mineral content of this marly sample. These compounds may originate from clay-catalysed sterane rearrangement during diagenesis (Peakman and Maxwell, 1988). The diasterane index C27Dia/(C27Dia+C29Sterane) values range from 0.15 to 0.59 (Fig. 9b; Table 5). With the exclusion of sample OBL4, the values correlate with those for the %ααS and %Ts (Table 4). The mature sample SM14 has a diasterane index value almost identical to that of the immature sample DOY4 (0.34 and 0.33, respectively; Fig. 9b; Table 5). This may be due to the occurrence of a more carbonate-rich facies at the Kalaat Senan locality.

6.3. Biomarkers OM source

The distribution of n-alkanes in crude oils and source rocks can be used to indicate the organic matter source (Tissot et al., 1977; Peters and Moldowan, 1993).

For immature to low mature samples, n-alkane distributions (Fig. 4) with a single mode maximizing in the n-C17 to n-C20 range and with a regular decrease towards the higher

homologues are consistent with a marine source of OM. The Bahloul Formation SHC revealed that the Pr (i-C19) is the most abundant isoprenoid compound in all samples (Fig. 4). If, as generally accepted, this represents a product of decarboxylation of phytanic acid (derived from phytol), the Pr/Ph ratio tends to be high in more oxidizing environments and low in strongly reducing ones (Powell and McKirdy, 1973). For example, bituminous coals and oils originating from higher plants are known to have higher Pr/Ph values than marine oils and sediments (5-10 vs. <1-3) (Powell, 1988). Marine organic-rich sediments and oils have a narrow range of Pr/Ph values (0.8-2.5; Tissot and Welte, 1984). However, the highest values, recorded in samples OBZ6 and OBZ8, may also at least partly represent chemical signatures of various Pr precursors (Powell, 1988; Philip, 1994), not only indicating an oxidizing environment or higher plant contribution. For the other samples, Pr/Ph values of 1-2.84 may indicate an algal and bacterial OM input under suboxic and anoxic depositional conditions.

The occurrence of C21-C25 acyclic isoprenoids in all samples (Fig. 6) suggests that the Pr/Ph values of the Bahloul Formation extracts were controlled both by source input and redox conditions. However, an increase of these values only takes place if the phytol of chlorophyll-a is the sole or at least the predominant source of isoprenoids (Brown and Kenig, 2004). The high values of Pr/n-C17 and Ph/n-C18 recorded in samples OBZ and AZ are consistent with multiple sources for these isoprenoids.

The regular steranes /17α(H)-hopanes ratio reflects input of eukaryotic (mainly algae and higher plants) versus prokaryotic (bacteria) organisms to the source rock (Chakhmakchev et al., 1996). The sterane/hopane ratio is relatively high in marine organic matter, with values generally approaching unity or even higher. In contrast, low steranes and sterane/hopane

ratios are more indicative of terrigenous and/or microbially reworked organic matter (Chakhmakchev et al., 1996).

The respective contributions of prokaryotic and eukaryotic organisms to the OM were estimated using the total terpanes/total steranes (TT/TS) ratio. TT here represents the sum of 17α(H),21β(H) C29 and C30 hopanes (m/z 191, Fig. 6), whereas TS has been estimated from the sum of the isomers retaining the biogenic configuration, i.e. 14α(H),17α(H)-20R (C27+C28+C29) (Fig. 6). TT/TS is also a facies parameter; a high value indicating a lacustrine or a bacteria-influenced facies, and a low value indicating an algal-dominated marine organic facies (Mackenzie et al., 1984). In the Bahloul Formation, values of the TT/TS ratio cover a wide from 1.2 to 5.33 (Table 5; Fig. 10a). High values suggest a high contribution of prokaryotic organisms (bacteria) to the OM. The TT/TS ratio appears to be consistent with %ααS which probably refers to the thermal alteration of the 20R steranes epimer and the concentration of the C29 and C30 hopane series. However, the high TT/TS and %ααS ratio values are both recorded in the immature sample OBL4 (Figs. 9a and 10a). At this locality these values could be consistent with high levels of bacterial activity (high TT) and the biodegradation of plankton remains (low TS). Bacterial recycling of planktonic OM occurred on the basin floor (Bechtel et al., 1996). Consequently, the TT/TS results do not indicate a reduced plankton contribution to the OM. Thus, planktonic biomass produced in the surface waters first undergoes degradation and mineralization in the water column, with a second cycle of degradation by "anaerobic" microorganisms (bacteria) at the sea floor.

6.4. Organic facies and early biodegradation of OM

The distribution of αα20R C27, C28 and C29 regular steranes can be used as a facies parameter (Shanmugam, 1985). Marine steranes are derived from the sterols of eukaryotes

such as diatoms, dinaflagellates, zooplankton and higher plants (de Leeuw et al., 1989). Samples OBL4, GH2, SM14 and OBZ5 show a slight dominance of the αα20R C29 sterane (39-41% of TS) over its C27 counterpart (34-38% of TS) (Fig. 10b, Table 5). The relative abundance of C27, C28 and C29 steranes is consistent with an open marine to estuarine algal-dominated organo-facies (Moldowan et al., 1985). The slightly prominent C29 sterane might indicate a land plant contribution to organic matter in the Bahloul Formation as assumed by Czochanska et al. (1988).

However, caution should be taken in interpreting the predominance of C29 steranes as a continental OM input (Volkman, 1988). For example, Palaeozoic oils from carbonate source rocks, with no or little higher plant contribution, show high concentrations of C29 steranes (Grantham, 1986b; Buchardt et al., 1989). Abundant C29 steranes can originate from particular bacteria which are able to synthesize this compound. In addition, in the case of partial biodegradation, the preferential sterane degradation order is C27> C28> C29 (Chosson et al., 1989) thus favouring the αα20R C29 steranes versus their C27 and C28 counterparts (Rullkötter and Wendisch, 1982). For Recent sediments, Freese et al. (2008) showed that bacteria rapidly degraded the labile OM of marine eukaryotic organisms during settling through the water column or at the sediment-water interface, and the OM developed a terrestrial-type signature (C29 >C27 steranes). As mentioned above, sterane biodegradation only occurs at an advanced stage, and directly after the removal of the regular isoprenoids (Peters and Moldowan, 1993).

In the present case, for sample OBZ5 only, alkane distributions show significant n-alkane reduction versus the isoprenoids Pr and Ph (Fig. 4). Therefore, the abundance of the αα20R C29 sterane in samples OBL4, GH2 and OBZ5 (Table 5; Fig. 6) can consistently be assigned

to a specific bacterial input together with selective early biodegradation of C27 steranes. Sample SM14 represents a more proximal setting with less C27 steranes being preserved.

6.5. Source rock palaeogeographic setting

None of the samples, recovered from a wide area in Tunisia, in terms of both their n-alkane and sterane and terpane distributions, indicate the occurrence of biomarkers diagnostic of higher plants (e.g. oleanane; Ekweozor et al., 1979; Moldowan et al., 1994). The samples were therefore deposited in palaeogeographic settings far from land (Fig. 1). The biomarker signatures are consistent with previous studies, notably of palynofacies (Caron et al., 1999), which showed that the OM is homogeneous and is dominated by amorphous marine algal or bacterial materials; palynomorphs of terrestrial origin (pollen and spores) and phytoclasts were only observed occasionally. However, the sporadic appearance of Botryococcus in the marly limestones suggests the influence of a brackish-water or lagoon environment (Caron et al., 1999). The sterane abundance in the formation is consistent with exclusively planktonic marine OM associated with a significant bacterial contribution. The thermal evolution as indicated by both Rock-Eval and biomarker maturity parameters is controlled by the structural setting and the proximity of the Triassic salt diapirs. At Garn Halfaya, Koudiat El Hamra and Oued Bazina, the immaturity of the OM coincides with the actual salt diapiric outcrops (diapir zone). Vertical halokinetic movements prevented the increased burial of the sediment. OM from outcrop sections located far from the Triassic diapirs was sufficiently deeply buried to generate hydrocarbons, as at the Kalaat Senan (SM), Jebel Ksikiss (JK) and Jebel Hadida (JH) locations in the west of the study area. For the Kalaat Senan locality, the relative abundance of tricyclic terpanes could indicate a more algal contribution and/or the thermal generation of these compounds.

7. CONCLUSIONS

The results indicate that there are significant variations in the quantity, composition and quality of organic matter in the Cenomanian-Turonian Bahloul Formation in central and northern Tunisia. The OM content of the formation was highest in the east of the study area, up to 18.7% TOC. All the other localities have average TOC values <2.4% range. These values suggest that the OM richness was controlled by the palaeogegraphic setting and structural style during sedimentation. The highest TOC values coincide with half grabens near the Jebel Serdj and Jebel Bargou highs and around local Triassic diapirs.

Rock-Eval Tmax values, Ts/(Ts+Tm) ratios, 22S/(22S+22R) values for C31 homohopanes, ββ/(ββ+αα)20R and 20S/(20S+20R) ratios for C29 steranes give consistent maturity indications for the eight sampled localities. They show that the Bahloul Formation OM has reached different stages of thermal maturity, but delineate a general east-to-west increasing maturity trend. Discrepancies in maturity were controlled by local palaeogeographic and structural features. Highest maturities were recorded in west Tunisia, indicating increased burial depths associated with a higher geothermal gradient. A greater algal contribution and a more proximal setting were suggested for the Kalaat Senan locality by the relatively high tricyclic terpanes/hopane ratio and the low diasterane index values.

The high values of Pr/Ph, Pr/n-C17 and Ph/n-C18 are characteristic of a suboxic to anoxic open-marine depositional setting and refer to the various isoprenoid precursors preserved in the EOM.

The study shows that terpanes are relatively more prominent than steranes in the organic matter, consistent with a major contribution by bacteria to the OM supply. The predominance of C29 over C27 steranes may be due to the early biodegradation of planktonic supply associated with specific bacterial contribution of steranes and may not necessarily imply a land plant contribution. OM content and biomarker signatures are consistent with the development of an oxygen minimum zone related to high surface bioproductivity and restricted circulation, associated with narrow half graben structures. At the water-sediment interface, high bacterial activity significantly contributed to the OM signature.

Acknowledgements

Financial support for this study was provided by the research unit "Georesources, Natural Environments and Global Changes" (GEOGLOB; code: 03/UR/10-02, Tunisia). The authors are deeply grateful to Habib Belayouni, Professor at the Faculty of Sciences of Tunis, University of Tunis El Manar, for his help and assistance with Rock-Eval pyrolysis and to Professor Monem Kallel, Director of the Research Laboratory of Environment Sciences (L.A.R.S.E.N., National School of Engineering of Sfax, University of Sfax) for his assistance with GC-MS analysis. We would like to thank anonymous reviewers for helpful reviews.

References

ABDALLAH, H., MEISTER, C. (1997) The Cenomanian–Turonian boundary in the Gafsa–Chott area (southern part of central Tunisia): biostratigraphy, palaeoenvironments. Cretaceous Research, 18, 197–236.

ABDALLAH, H., MEMMI, L., DAMOTTE, R., RAT, P., MAGNIEZ-JANNIN, F. (1995) Le Crétacé de la chaîne nord des Chotts (Tunisie du centre-sud): biostratigraphie et comparaison avec les régions voisines. Cretaceous Research, 16, 487–538.

ABDALLAH, H., SASSI, S., MEISTER, C., SOUISSI, R. (2000) Stratigraphie séquentielle et paléogéographie à la limite Cénomanien–Turonien dans la région de Gafsa-Chotts (Tunisie centrale). Cretaceous Research, 21, 35–106.

AFFOURI, H. 1996 Contribution à l'étude comparative des matières organiques associées aux faciès "roches mères de pétrole" d'âges Cénomano-Turonien (Bahloul) et Yprésien (Bou Dabbous) en Tunisie centro-septentrionale : conséquences géochimiques et implications pétrolières. Mémoire de Diplôme d'Etudes Approfondies, Université Tunis II, Faculté des Sciences de Tunis.

AFFOURI, H. (2004) Etude géochimique des faciès roches mères d'hydrocarbures et réservoirs potentiels dans le cadre de l'exploration pétrolière en Tunisie septentrionale. Thèse de Doctorat, Université de Tunis El Manar, 219p.

ANDERSON, J. E. (1991) Subsidence history and structural evolution of the western margin of the Pelagian Platform, central Tunisia. Ph.D Thesis, Kingston University, UK.

BECHTEL A., SHIEH, Y-N., PERVAZ, M., PÜTTMANN, W. 1996 Biodegradation of hydrocarbons and biogeochemical sulfur cycling in the salt dome environment: Inferences from sulfur isotope and organic geochemical investigations of the Bahloul Formation at the Bou Grine Zn/Pb ore deposit, Tunisia. Geochimica et Cosmochimica Acta, 60, 2833-2855.

BECHTEL, A., PEVAZ, M., PÜTTMANN, W. (1998) Role of organic matter and sulphate-reducing bacteria for metal sulphide precipitation in the Bahloul Formation at the Bou Grine Zn/Pb deposit (Tunisia). Chemical Geology, 144, 1–21.

BEDIR, M., BOUKADI, N., TLIG, S., TIMZAL, F.B., ZITOUNI, L., ALOUANI, R., SLIMANE, F., BOBIER, C., ZARGOUNI, F. (2001) Subsurface Mesozoic basins in the central Atlas of Tunisia: tectonics, sequence deposit distribution, and hydrocarbon potential. AAPG Bull., 85(5), 885–907.

BELAYOUNI, H., CHANDOUL, H., M'RAD, R. (1992) Oil seeps and associated phenomena in northern Tunisia. Field trip guide book, IIIe Journées d'exploration pétrolière en Tunisie, Entreprise Tunisienne d'Activités Pétrolières (Eds.), Tunis.

BEN DHIA, H. (1987) The geothermal gradient map of Central Tunisia: Comparison with structural, gravimetric and petroleum data. Tectonophysics, 142, 99-109.

BEN FERJANI, A., BUROLLET, P.F., MEJRI, F. (1990) Petroleum Geology of Tunisia. Entreprise Tunisienne d'Activités Pétrolières (Eds.), Tunis.

BEN HADJ ALI, N., RAZGALLAH S., BEN HADJ ALI, M., KENNEDY, J.W. (1994) La Formation Bahloul dans sa localité type: précisions stratigraphiques basées sur les ammonites et les foraminifères planctoniques. Notes Service Géologique de la Tunisie, 60, 35-69.

BENNETT, B., OLSEN, S.D. (2007) The influence of source depositional conditions on the hydrocarbons and nitrogen compounds in petroleum from central Montana, USA. Organic Geochemistry, 38, 935-956.

BAIRD, A.W., GROCOTT, J., SANDMAN, R.I., GRANT, G.G., MOODY, R.T.J. (1990) A radial reinterpretation of the Tunisian Atlas thrust belt and foreland basin system. International Conference on Thrust Tectonics, Royal Holloway and Bedford New College. Program and Abstracts, 81.

BISHOP, W.F. (1988) Petroleum Geology of the East-Central Tunisia. AAPG Bull., 72, 1033-1058.

BOCCALETTI, M., CELLO, G., TORTORICI, L. (1988) Structural and tectonic significance of the North-South axis of Tunisia. Annales Tectonicae, 2, 12-20.

DURAND, B. (1993) Composition and structure of organic matter in immature sediments. In: BORDENAVE, M.L. (Ed.), Applied Petroleum Geochemistry, Éditions Technip, Paris, 77-100.

BOYER, S. E., ELLIOT, D. (1982) Thrust systems. AAPG Bull., 66, 1196-1230.

BRIGGS, J.R. (2007) Influence of climate and hydrology on carbon in an early Miocene peat land. PhD Thesis, Univ. Nottingham, 267 pp.

BROWN, T.C., KENIG, F. (2004) Water column structure during deposition of Middle Devonian – Lower Mississippian black and green/gray shales of the Illinois and Michigan Basins: a biomarker approach. Palaeogeography, Palaeoclimatology, Palaeoecology, 215, 59-85.

BUCHARDT, B., CHRISTIANSEN, F.G., NOHR-HANSEN, H., LARSEN, N. H., OSTFELDT P. (1989) Composition of organic matter in source rocks. In: Christiansen, F.G. (ed.) Petroleum Geology of North Greenland. Grønlands Geologiske Undersøgelse Bulletin, 158, 32-39.

BUROLLET, P.F., DESFORGE, G. (1982) Dynamique des bassins néocrétacés en Tunisie. Mémoire Géologique, Université de Dijon, 7, 381-389.

BUROLLET, P.F. (1956) Contribution à l'étude stratigraphique de la Tunisie Centrale. Annales des Mines et de la Géologie, Tunisie, 18, 1–345.

CAMOIN, G.F. (1991) Sedimentologic and paleotectonic evolution of carbonate platforms on a segmented continental margin: example of the African Tethyan margin during Turonian and Early Senonian times. Palaeogeography Palaeoclimatology Palaeoecology, 87, 29–52.

CARON, M., ROBASZYNSKI, F., AMEDRO, F., BAUDIN, F., DECKONINK, J. F., HOCHULI, P., SALIS PERCH NIELSEN, K. (VON), TRIBOVILLARD N. (1999) Estimation de la durée de l'événement anoxique global au passage Cénomanien Turonien.

Approche cyclostratigraphique dans la Formation Bahloul en Tunisie centrale. Bull. soc. Géol. Fr., 170, 145–160.

CARON, M., DALL'AGNOLO, S., ACCARIE, H., BARRERA, E., KAUFFMAN, E.G., AMÉDRO, F., ROBASZYNSKI, F. (2006) High-resolution stratigraphy of the Cenomanian–Turonian boundary interval at Pueblo (USA) and Wadi Bahloul (Tunisia): stable isotope and bio-events correlation. Geobios, 39, 171–200.

CHAABANI, F., RAZGALLAH, S., DONZE, P., BELAYOUNI, H. (1994) L'épisode anoxique du passage Cénomanien-Turonien au Jebel Berda (Tunisie centro-méridionale): stratigraphie et géochimie. Notes du Service Géologique de Tunisie, 60, 21–33.

CHAKHMAKCHEV, A., SUZUKI, N., SUZUKI, M., TAKAYAMA, K. (1996) Biomarker distributions in oils from the Akita and Niigata Basins, Japan, Alexander Chekhmakhchey. Chemical geology, 133, 1-14.

CHOSSON, P., CONNAN, J., DESSORT, D. (1989) In vitro biodegradation of steranes and terpanes: A clue to understanding geological situations. In: J. Moldowan, J. M., Albrecht, P., Philp, R. P. (ed.) Biological Markers in Sediments and Petroleum. Prentice Hall, Englewood Cliffs, N. J., 320-349.

CONNAN, J. (1984) Biodegradation of crude oils in reservoirs. In: Brooks, J., Welte, D.H. (ed.) Advances in Petroleum Geochemistry No 1. Academic Press, New York, 299-335.

CONNAN, J., RESTLÉ, A., ALBRECHT, P. (1980) Biodegradation of crude oil in the Aquitaine basin. In: Douglas A.G., Maxwell J.R. (ed.) Advances in Organic Geochemistry 1979. Pergamon Press, Oxford, 1−17.

CORNFORD, C. (1986) Source rocks and hydrocarbons of the North sea. In: Glennie, K.W. (ed.) Introduction to the Petroleum Geology of the North Sea. Oxford, U.K., 197-236.

CZOCHANSKA, Z., GILBERT, T.D., PHILP R.P., SHEPPARD, C.M., WESTON, R.J., WOOD, T.A., WOOLHOUSE, A.D. (1988) Geochemical application of steranes and

triterpanes biomarkers to a description of oils from Taranaki Basin in New Zealand. Organic Geochemistry, 12, 123-135.

DAHL, J., MOLDOWAN, J.M., SUNDARARAMAN, P. (1993) Relationship of biomarker distribution to depositional environment: Phosphoria Formation, Montana, USA. Organic Geochemistry, 20, 1001–1007.

DE GRANDE, S.M.B., AQUINO NETO, F.R., MELLO, M.R. (1993) Extended tricyclic terpanes in sediments and petroleum. Organic Geochemistry, 20, 1039-1047.

DE LEEUW, J.W, COX, H.C., VAN GRAAS, G., VAN DE MEER, F.W., PEAKMAN, T. M., BAAS, J.M. A., VAN DE GRAAF, V. (1989) Limited double bond isomerization and seletive hydrogenation of sterenes during early diagenesis. Geochimica and Cosmochimica Acta, 53, 903-909.

EGLINTON, G., CALVIN, M., 1967. Chemical fossils. Scientific American, 261, 32-43.

EKWEOZOR, C.M., STRAUSZ, O.P. (1982) 18,19-Bisnor-13βH, 14-αH-cheilanthane: a novel degraded tricyclic sesterterpenoid-type hydrocarbon from the Athabasca oil sands. Tetrahedron Letters, 23, 2711-2714.

EKWEOZOR, C.M., OKOGUN, J.I., EKONG, D.E.U., MAXWELL, J.R. (1979) Preliminary organic geochemical studies of samples from the Niger delta (Nigeria): II. Analyses of shale for triterpenoid derivatives. Chemical Geology, 27, 1-2, 29-37.

ESPITALIÉ, J., DEROO, G., MARQUIS, F. (1985) La pyrolyse Rock–Eval et ses applications (deuxième partie). Revue de l'Institut Français du Pétrole, 40, 755–784.

ESPITALIÉ, J., LAPORTE, J. L., MADEC, M., MARQUIS, F., LEPLAT, P., PAULET, J., BOUTEFEU, A. (1977) Méthode rapide de caractérisation des roches mètres, de leur potentiel pétrolier et de leur degré d'évolution. Revue de l'Institut Français du Pétrole, 32, 23–42.

FICKEN, K.J., WOLLER, M.J., SWAIN, D.L. (2002) Reconstruction of a subalpine grass-dominated ecosystem, Lake Rutundu, Mount Kenya: a novel multi-proxy approach. Pales, 177, 137-149.

FREESE, E., KÖSTER, J., RULLKÖTTER, J. (2008) Origin and composition of organic matter in tidal flat sediments from the German Wadden Sea. Organic Geochemistry, 39, 820–829.

GAAYA, A., GHENIMA, R. (1998) Major and potential petroleum systems in Tunisia. Prospectivity and expectations. In: Proceedings of the 6th Tunisian Petroleum Exploration and Production Conference, Tunis 5– 9 May 1998. Entreprise Tunisienne d'Activités Pétrolières (ed.) Memoir, 12, 169– 177.

GOOSSENS, H., DE LEEUW, J.W., SCHENCK, P.A., BRASSELL, S.C. (1984) Tocopherols as likely precursors of pristane in ancient sediments and crude oils. Nature, 312, 440-442.

GRACIANSKY, P.C., BROSSE, E., DEROO, G., HERBIN, J. P., MONTADERT, L., MÜLLER C., SCHAAF, A., SIGAL, J. (1982) Les formations d'âge Crétacé de l'Atlantique Nord et leur matière organique : Paléogéographie et milieu de dépôts. Revue de l'Institut Français du Pétrole, 37, 275-336.

GRANTHAM, P. J. (1986a) Sterane isomerization and moretane/hopanes ratios in crude oils derived from tertiary source rocks. Organic Geochemistry, 9, 293-304.

GRANTHAM, P. J. (1986b) The occurrence of unusual C27 and C29 steranes predominances in two types of Oman crude oil. Organic Geochemistry, 9, 1-10.

GRASSO, M., TORELLI, L., MAZZOLDI, G. (1999) Cretaceous–Palaeogene sedimentation patterns and structural evolution of the Tunisian shelf, offshore the Pelagian islands (central Mediterranean). Tectonophysics, 315, 235– 250.

GUIRAUD, R., MAURIN, J.E. (1991) Le rifting en Afrique au Cretace inferieur: synthese structurale, mise en évidence de deux étapes dans la genèse des bassins, relations avec les ouvertures océaniques péri-africaines. Bull. Soc. Geol Fr., 162, 811-823.

HU MING-AN, DISNAR, J. R., SUREAU, J.-F. (1995) Organic geochemical indicators of biological sulfate reduction in early diagenetic Zn-Pb mineralisation: the Bois-Madame deposit (Gard, France). Applied Geochemistry, 10, 419-435.

HUGHES, W.B., REED, J.D. (1995) Oil and source rock geochemistry and exploration implications in northern Tunisia. In: Proceedings of the seminar on source rocks and hydrocarbon habitat in Tunisia. Entreprise Tunisienne d'Activités Pétrolières (ed.), Tunis. Memoir, 9, 49-67.

HUNT, J.M. (1995) Petroleum Geochemistry and Geology. Freeman, W.H., and Company, New York, 743p.

IBOUH, H., ZARGOUNI, F. (1998) Nouvelles données sur la tectonique synsédimentaire du Crétace inférieur et le début du Crétacé supérieur au niveau de la jonction des Jebels Orbata et Bouhedma (Tunisie meridionale). African Geosciences Revue, 5, 207–215.

JARVIE, D. M. (1991) Total organic carbon (TOC) analysis. In: Merrill, R. K. (ed.) Treatise of petroleum geology: Handbook of petroleum geology, source and migration processes and evaluation techniques. AAPG Bull., 113–118.

JEFFERIES, R., MILTON, P. (1965) The mode of life of two Jurassic species of "Posidonia" (Bivalvia). Palaeontology, 8, 156–185.

KRUGE, M.A., HUBERT, J.F., AKES, R.J., MERINEY, P.E. (1990) Biological markers in lower Jurassic synrift lacustrine black shales, Hartford Basin, Connecticut, USA. Organic Geochemistry, 15, 281–289.

LAYEB, M., JOUIROU, M., BELAYOUNI, H. (2001) Signification du contenu argileux de la formation Bahloul. Notes du Service Géologique de Tunisie, 67, 5-12.

LAYEB, M., BELAYOUNI, H. (1991) Géologie et géochimie de la Formation Bahloul (Cénomanien-Turonien) en Tunisie nord-centrale. Séminaire sur les Evénements du Cénomanien et du Turonien, Tunis, 1991. Association Tunisienne des Etudes Internationales en Géologie (ed.). Résumé, 12-14.

LAYEB, M., BELAYOUNI, H. (2000) Paléogéographie de la Formation Bahloul (passage Cénomanien – Turonien). Annales des Mines et de la Géologie, Tunisie, 40, 21-44

LAYEB, M., 1990. Etude géologique, géochimique et minéralogique régionale des faciès riches en matière organique d'âge Cénomano-Turonien dans le domaine de la Tunisie nord-centrale. Thèse de Doctorat de Spécialité Géologie. Univ. Tunis II.

LÜNING S., KOLONIC, S, BELHADJ, E.M., BELHADJ, Z., COTA, L., BARIC, G., WAGNER, T. (2004) Integrated depositional model for the Cenomanian–Turonian organic-rich strata in North Africa. Earth-Science Reviews, 64, 51– 117

MAAMOURI, A.L., ZAGHBIB-TURKI, D., MATMATI, M.F., CHIKHAOUI, M., SALAJ, J. (1994) La Formation Bahloul en Tunisie centro-septentrionale: variations latérales, nouvelle datation et nouvelle interprétation en terme de stratigraphie séquentielle. Journal African Earth Science, 18, 37–50

MACKENZIE, A.S., MAXWELL, J.R., COLEMAN, M.L., DEEGAN, C.E. (1984) Biological markers and isotope studies of North Sea crude oils and sediments. Proceedings of the 11th World Petroleum Congress, 2, Wiley, New York, 45-56.

MACKENZIE, A.S., PATIENCE, R.L., MAXWELL, J.R., VANDENBROUCKE, M., DURAND, B. (1980) Molecular parameters of maturation in the Toarcian shales, Paris basin, France I. Changes in the configurations of the acyclic isoprenoid alkanes, steranes and triterpanes. Geochimica et Cosmochimica Acta, 44, 1709–1721.

MAURIN, J.C., GUIRAUD, R. (1993) Basement control in the development of the Early Cretaceous West and Central African Rift System. Tectonophysics, 228, 81–95.

MOLDOWAN, J. M.; SUNDARARAMAN, P., SCHOELL, M. (1986) Sensitivity of biomarker properties to depositional environment and/or source input in the Lower Toarcian of S.W. Germany. Organic Geochemistry, 10, 915-926.

MOLDOWAN, J.M., DAHL, J., HUIZINGA, B., FAGO, F. (1994) The molecular fossil record of oleanane and its relation to angiosperms. Science, 265, 768-771.

MOLDOWAN, J.M., SEIFERT, W.K., GALLEGOS, E.J. (1985) Relationship between petroleum composition and depositional environment of petroleum source rocks. AAPG Bull., 69, 1255-1268.

MONTACER, M. (1995) Comparative organic geochemistry of two Tunisian oil source rocks (Bahloul and Bou Dabbous) as an approach of oil exploration in the northern part of Tunisia. In: Entreprise Tunisienne d'Activités Pétrolière (ed.).Proceeding of the seminar on source rocks and hydrocarbons habit in Tunisia, Memoir, 9, 49-67.

MONTACER, M. (1991) Apport de l'étude de la matière organique à la compréhension de la genèse des sulfures de Zn-Pb associés aux faciès carbonatés de la Formation « Bahloul » (Cénomano-turonien) de Bou Grine. Séminaire sur les Evénements du Cénomanien et du Turonien, Association Tunisienne des Etudes Internationales de Géologie, volume des communications, 17-21.

MONTACER, M. (1989) Etude de la matière organique de la Formation "Bahloul" (Cénomanien-Turonien) dans l'environnement sédimentaire du gisement Zn-Pb de Bou Grine (NW de la Tunisie). Thèse d'Etat, Université Orléans, France.

MONTACER, M., DISNAR, J.R., ORGEVAL, J.J., TRICHET, J. (1988) Relationship between Zn –Pb ore and oil accumulation processes: Example of the Bougrine deposit (Tunisia). Organic Geochemistry, 13, 423–431.

MORGAN, M.A., GROCOTT, J., MOODY, R.T.J. (1998) The structural evolution of the Zaghouan-Ressas Structural Belt, northern Tunisia. In: Macgregor, D.S.; Moody, R.T.J.

and Clark-Lowes, D.D. (ed.) Petroleum geology of North Africa. Geological Society, London, Special Publication, 132, 405–422.

ORGEVAL, J.J. (1994) Peridiapiric Metal Concentration: Example of the Bou Grine deposit (Tunisian Atlas). In: Fontboté/Boni (ed.) Sediment-Hosted Zn–Pb Ores. Springer, Berlin, 354–389.

OURISSON, G., ALBRECHT, P., ROHMER, M. (1982) Predictive microbial biochemistry from molecular fossils to procaryotic membranes. Trends in Bio-Sciences, 236-239.

PATRIAT, M., ELLOUZ, N., DEY, Z., GAULLIER, J.M. and BEN KILANI, H. (2003) The Hammamet, Gabes and Chotts basins (Tunisia): a review of the subsidence history. Sedimentary Geology, 156, 241-262.

PEAKMAN, T.M., MAXWELL, J.R. (1988) Early diagenetic pathways of steroid alkenes. Organic Geochemistry, 13, 583–592.

PERTHUISOT, V. (1981) Diapirism in northern Tunisia. Journal of Structural Geology, 3, 231-235.

PERTHUISOT, V. (1978) Dynamique et pétrogenèse des extrusions triasiques en Tunisie septentrionale. Travaux du Laboratoire de Géologie (ed.) Presses E.N.S., Paris, 12, 312 p.

PETERS, K. E., CASA, M. R. (1994) Applied source rock geochemistry. In: Magoon, L. B. and Dow, W. G. (ed.) The petroleum system–from source to trap. AAPG Bull., 60, 93-120.

PETERS, K.E., MOLDOWAN, J.M. (1993) The Biomarker Guide: Interpreting Molecular Fossils in Petroleum and Ancient Sediment. Prentice Hall, Englewood Cliffs, NJ, 347 p.

PETERS, K.E. (1986) Guidelines for evaluating petroleum source rocks using programmed pyrolysis. AAPG Bull., 70, 318-329.

PETERS, K.E., FRASER, T.H., AMRIS, W., RUSTANTO, B., HERMANTP, E. (1999) Geochemistry of crude oils from eastern Indonesia. AAPG Bull., 83, 1927–1942.

PETERS, K.E., MOLDOWAN, J.M. and SUNDARARAMAN, P. (1990) Effects of hydrous pyrolysis on biomarker thermal maturity parameters: Monterey Phosphatic and Siliceous members. Organic Geochemistry, 15, 249-265.

PHILIP, R.P. (1994) Geochemical characteristics of oil derived predominantly from terrigenous source material. In: Scott, A.C and Fleet, A.J. (ed) Coal and coal bearing strata as oil prone source rocks. Geol. Soc. Spec. Publ., London, 77, 71-91.

POWELL, T.G. (1988) Pristane/phytane ratio as environmental indicator. Nature, 333, 604.

POWELL, T.G., MCKIRDY, D.M. (1973) Relationship between ratio of pristane to phytane, crude oil composition and geological environment in Australia. Nature, 243, 37-39.

RAZGALLAH, S., PHILIP, J., THOMEL, G., ZAGHBIB-TURKI, D., CHAABANI, F., BEN HAJ ALI, N., M'RABET, A. (1994) La limite Cénomanien–Turonien en Tunisie centrale et méridionale: biostratigraphie et paléoenvironnements. Cretaceous Research, 15, 507–533.

REQUEJO, A. G., HALPERN, H. I. (1989) An unusual hopane biodegradation sequence in tar sands from the Pt Arena (Monterey) Formation. Nature, 342, 670- 673

REVILL, A.T., VOLKMAN, J.K., O'LEARY, T., SUMMONS, R.E., BOREHAM, C.J., BANKS, M.R., DENWER, K. (1994) Hydrocarbon biomarkers, thermal maturity, and depositional setting of tasmanite oil shales from Tasmania, Australia. Geochimica et Cosmochimica Acta, 58, 3803-3822.

ROBASZYNSKI, F., AMÉDRO, F., CARON, M. (1993). La limite Cénomanien–Turonien et la Formation Bahloul dans quelques localités de Tunisie Centrale. Cretaceous Research, 14, 477–486.

ROBASZYNSKI, F., CARON, M., AMEDRO, F., DUPUIS, C., HARDENBOL, J., GONZALEZ DONOZO, J.M., LINARES, D., GARTNER, S. (1993b) Le Cénomanien de la région de Kalaat Senan (Tunisie centrale): lithostratigraphie et interprétation séquentielle. Revue de Paléontologie, 12, 351-505.

ROBASZYNSKI, F., HARDENBOL, J., CARON, M., AMÉDRO, F., DUPUIS, C., GONZALEZ DONOSO, J.-M., LINARES, D., GARTNER, S. (1993c) Sequence stratigraphy in a distal environment: the Cenomanian of the Kalaat Senan region (central Tunisia). Bulletin des Centres de Recherches Exploration-Production Elf Aquitaine, 17, 395– 433.

ROBASZYNSKI, F., CARON, M., DUPUIS, C., AMEDRO, F., GONZALEZ DONOSO, J.-M., LINARES, D., HARDENBOL, J., GARTNER, S., CALANDRA, F., DELOFFRE, R. (1990) A tentative integrated stratigraphy in the Turonian of central Tunisia: Formations, zones and sequential stratigraphy in the Kalaat Senan area. Bulletin des Centres de Recherches Exploration-Production Elf Aquitaine, 14, 213–384.

ROUSHDY, M. I.; EL NADY, M.M.; MOSTAFA, Y. M.; EL GENDY, N.SH., ALI, H. R. (2010) Biomarkers Characteristics of Crude Oils from some Oilfields in the Gulf of Suez, Egypt. Journal of American Science, 6, 911-925.

ROUVIER, H. (1977) Géologie de l'extrême-nord tunisien: tectoniques et paléogéographies superposées à l'extrémité orientale de la chaîne nord-maghrébine. Thèse Sci. Univ. Paris VI.

RULLKÖTTER, J., WENDISCH, D. (1982) Microbial alteration of 17α(H)-hopane in Madagascar asphalts : Removal of C-10 methyl group and ring opening. Geochimica et Cosmochimica Acta, 46, 1543-1553.

SALAJ, J. (1976) Contribution à la microbiostratigraphie du Mésozoique et du Tertiaire de Tunisie septentrionale. Notes du Service Géologique de Tunisie, 42, 29-69.

SCHLANGER, S.O., ARTHUR, M.A., JENKYNS, H.C., SCHOLLE, P.A. (1987a) The Cenomanian–Turonian oceanic anoxic event: I. Stratigraphy and distribution of organic-rich beds and the marine δ13C excursion. In: Brooks, J., Fleet, A.J. (Eds.), Marine and Petroleum Source Rocks. Geol. Soc. Spec. Publ., London, 26, 371– 399.

SCHLANGER, S.O., ARTHUR, M.A., JENKYNS, H.C., SCHOLLE, P.A. (1987b) The Cenomanian/Turonian anoxic event deposits. In: Einsele, G., Seilacher, A. (ed.) Cyclic and Event Stratification. Springer-Verlag, New York, 161-173.

SEIFERT, W.K., MOLDOWAN, J.M. (1986) Use of biological markers in petroleum exploration. In: Johns, R.B. (ed.) Methods in Geochemistry and Geophysics, 24, 261-290.

SEIFERT, W.K., MOLDOWAN, J.M. (1981) Paleoreconstruction by biological markers. Geochimica et Cosmochimica Acta, 45, 783-794.

SEIFERT, W.K., MOLDOWAN, J.M. (1980) The effect of thermal stress on source-rock quality as measured by hopane stereochemistry. In: Douglas A.G., Maxwell J.R. (ed.) Advances in Organic Geochemistry 1979. Pergamon Press, Oxford, 229-237.

SEIFERT, W.K., MOLDOWAN, J.M., DEMAISON G.J. (1984) Source correlation of biodegraded oils. Organic Geochemistry, 6, 633-643.

SHANMUGAM, G. (1985) Significance of coniferous rain forest and related organic matter in generating commercial quantities of oil, Gippsland Basin, Australia. AAPG Bull., 69, 1241-1254.

SIERRA, M.G., CRAVERO, R.M., LABORDE, M.A., RUVEDA, E.A. (1984) Stereoselective synthesis of (+/-)-18,19-Dinor-13β(H)-cheilanthane: the most abundant tricyclic compound from petroleum and sediments. Journal of the Chemical Society, Chemical Communications, 417-418.

SNOCK, A. W., SCHAMEL, S., KARASEK, R. M. (1988) Structural evolution of Jebel Debadib Anticline: a clue to the regional tectonic style of the Tunisian Atlas. Tectonics, 7, 497-516.

SOUA, M. (2010) Productivity and bottom water redox conditions at the Cenomanian-Turonian Oceanic Anoxic Event in the southern Tethyan margin, Tunisia. Revue Méditerranéenne de l'Environnement, 4, 653-664.

SOUA, M., TRIBOVILLARD, N. (2007) Modèle de sédimentation au passage Cénomanien/Turonien pour la Formation Bahloul en Tunisie. Comptes Rendus Geoscience, 339, 692–701

SOUA, M., ECHIHI, O., HERKAT, M., ZAGHBIB-TURKI, D., SMAOUI J., FAKHFAKH-BEN JEMIA, H., BELGHAJI H. (2009) Structural context of the paleogeography of the Cenomanian-Turonian anoxic event in the eastern Atlas basins of the Maghreb. Comptes Rendus Geoscience, 341, 1029–1037.

SOYER, C., TRICART, P. (1989) Tectonique d'inversions en Tunisie centrale : le chaînon atlasique Segdal-Boudinar. Bull. Soc. Geol. Fr., 8, 829–836.

TISSOT, B., WELTE, D. H. (1984) Petroleum Formation and Occurrence - A new approach to oil and gas exploration. 2nd Ed. Springer, Berlin, 699 p.

TISSOT, B., PELET, R., ROUACH J., COMBAZ, A. (1977) Utilisation des alcanes comme fossiles géochimiques indicateurs des environnements géologiques. AAPG Bull., 55, 2177-2193.

TISSOT, B., DURAND, B., ESPITALIE, J., COMBAZ, A. (1974) Influence of the nature and diagenesis of organic matter in the formation of petroleum. AAPG Bull., 58, 499-506.

TISSOT, B., CALIFET-DEBYSER, Y., DEROO, G., OUDIN, J.L. (1971) Origin and evolution of hydrocarbons in early Toarcien shales, Paris Basin, France. AAPG Bull., 55, 2177-2193.

TURKI, M.M. (1985) Polycinématique et contrôle sédimentaire associé sur la cicatrice Zaghouan-Nebhana. Thèse Doc. Etat, Univ. Tunis, 228 p.

VILA, J.-M., BEN YOUSSEF, M., BOUHLEL, S., GHANMI, M., KASSA, S., MIAADI, F. (1995). Tectonique en radeaux au toit d'un « glacier de sel » sous-marin albien de Tunisie du Nord-Ouest: exemple du secteur minier de Gueurn Halfaya. Comptes Rendus de l'Académie des Sciences, IIA, 327, 563-570.

VILA, J.-M., BEN YOUSSEF, M., CHARRIERE, A., CHIKHAOUI, M., GHANMI, M., KAMOUN, F., PEYBERNES, B., SAADI, J., SOUQUET, P., ZARBOUT, M. (1994) Découverte en Tunisie, au SW du Kef, de matériel triasique interstratifié dans l'Albien : extension du domaine à glaciers de sel sous-marins des confins algéro-tunisiens. Comptes Rendus de l'Académie des Sciences, II, 318, 1661–1667.

VOLKMAN, J.K. (1988) Biological marker compounds as indicators of the depositional environments of petroleum source rocks. In: Fleet, A.J., Kelts, K., Talbot, M.R. (ed.) Lacustrine Petroleum Source Rocks. Geol. Soc. London, Spec. Publ., 40, 103-122.

YUKLER, M.A., MOUMEN, A., DAADOUCH, I., BOUHLEL, H., MESKINI, A., SAIDI, M., JARRAYA, H. (1994) Quantitative evaluation of the geologic and hydrocarbon potential of the Gulf of Gabès. In: Entreprise Tunisienne d'Activités Pétrolières (ed.) Proceedings of the 4th Tunisian Petroleum Exploration Conference, Tunis. Memoir, 8, 69–70.

ZAGRARNI, M.F., NEGRA, M.H., HANINI, A. (2008) Cenomanian–Turonian facies and sequence stratigraphy, Bahloul Formation, Tunisia. Sedimentary Geology, 204, 18–35

ZARGOUNI, F. (1985) Tectonique de l'Atlas méridional de Tunisie, évolution géométrique et cinématique des structures en zone de cisaillement. Revue Sciences de la Terre, INRST (ed.), Thèse Doctorat ès-Sc., Université Louis Pasteur, Strasbourg, France, Tunisie.

ZARGOUNI, F. (1975) Etude géologique de la chaîne de Lansarine (région de Tébourba, Atlas tunisien). Thèse de 3ème cycle. Univ. Pierre et Marie-Curie, Paris VI.

FIGURES AND TABLES CAPTION

Fig. 1. Sample location, Tunisian structural units, palaeogeography, facies and isopach map of Cenomanian-Turonian Bahloul Formation and its equivalent units in Tunisia (modified after Burollet, 1956; Perthuisot, 1981; Bishop, 1988; Boccaletti et al., 1988; Baird et al., 1990; Ben Ferjani et al., 1990; Anderson, 1991; Camoin, 1991; Orgeval, 1994; Grasso et al., 1999; Lüning et al., 2004). [OBL, Oued Bahloul; AZ, Ain Zakkar; DOY, Dyr Ouled Yahia; SM, Kalaat Senan; GH Garn El Halfaya; JK, Jebel Ksikiss; KEH, Koudiat El Hamra; MR, Koudiat Mghoutti Rassou; JH Jebel Hadida; 7KT, Jebel Sabaa Koudiat; OBZ, Oued Bazina].

Fig. 2. Bahloul Formation OM typing from samples investigated based on Rock-Eval Hydrogen Index vs. Tmax crossplot (HI, mgHC/g TOC; Tmax,°C).

Fig. 3. Petroleum potential of the Bahloul Formation [EOM, extractable organic matter (ppm/rock); TOC, Rock-Eval total organic carbon (% rock)].

Fig. 4. GC chromatograms of saturated hydrocarbons (SHCs) extracted from selected Bahloul Formation samples in central and northern Tunisia (numbers refer to n-alkanes; 17, n-heptadecane; 18, n-octadecane; Pr, pristane; Ph, phytane).

Fig. 5. Location of representative Bahloul Formation samples on a cross-plot of Pr/n-C17 versus Ph/n-C18 (Pr/n-C17: pristane/n-heptadecane peak height ratio; Ph/n-C18: phytane/n-octadecane peak height ratio.

Fig. 6. GC-MS chromatograms showing distribution of steranes (m/z 217) and triterpanes (m/z 191) of representative samples from the Bahloul Formation in central and northern Tunisia (for key see Table 3).

Fig. 7. Regional distribution of TOC average content of the Bahloul Formation in central and northern Tunisia [TOC, Rock-Eval total organic carbon (% rock)].

Fig. 8. Regional distribution of (a) Tmax., (b) HI, (c) %22SC31 and (d) Ts/Ts+Tm.
[Tmax (°C); HI, mgHC/g TOC; %22SC31, 22S x 100/(22S+22R) C31-homohopanes; Ts/Ts+Tm, 18α(H)-22,29,30-trinorneohopane x 100/ (18α(H)-22,29,30-trinorneohopane+ 17α(H)-22,29,30-trinorhopane)]

Fig. 9. Maturity biomarker distribution for Bahloul Formation OM (a) % □□20S-C29 sterane and (b) diasteranes index. For key see Tables 3 and 4.

Fig. 10. Regional distribution of (a) total terpanes/total steranes (TT/TS) and (b) relative abundance of regular 14α(H),17α(H)20R-(C27 and C29) steranes.
[%C27αα20R, αα20R-C27 steranes x 100/(αα20R-C27+ αα20R-C28+ αα20R-C29)steranes; %C29, αα20R-C29 steranes x 100/(αα20R-C27+ αα20R-C28+ αα20R-C29)steranes]. For key see Tables 3 and 4.

Table 1. Rock-Eval II (Espitalié et al., 1985) analysis of Cenomanian-Turonian Bahloul Formation samples from central and northern Tunisia.

Table 2. Bulk data for solvent extraction and chromatographic characterisation of Bahloul Formation samples from central northern Tunisia.

Table 3. Peak assignment for steranes (m/z 217) and triterpanes (m/z 191) in GC-MS chromatograms (Fig. 6).

Table 4. Triterpane results from GC-MS analysis of Bahloul OM in central and northern Tunisia (m/z 191).

Table 5. Sterane results from GC-MS analysis of Bahloul OM in central and northern Tunisia (m/z 217).

Figure 1

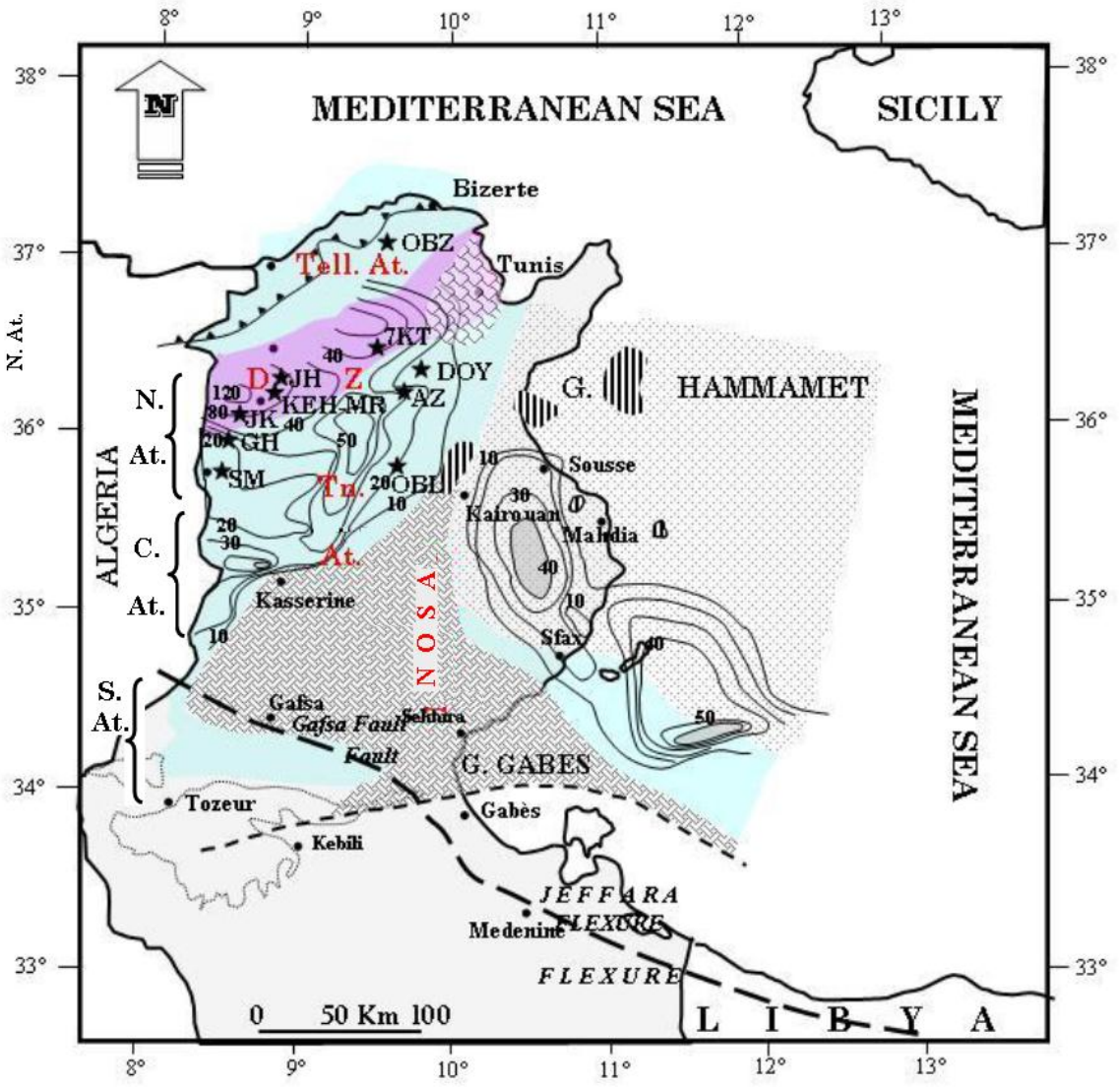

Legend:

Bahloul Fomation organic rich

Dolomite + Anhydrite

Rudist Bioaccumulation

Lagoon/Non Deposition continental

Bahloul Formation absent

Bahloul Formation organic poor

Tell. At., Tellian Atlas Zone;

DZ, Diapirs Zone; Tn. At., Tunisian Atlas [N., Northern; C., Central; S., Southern]; NOSA, North-South Axis (NOSA);

Isopach 10m; ★ Analysed section

Figure 2

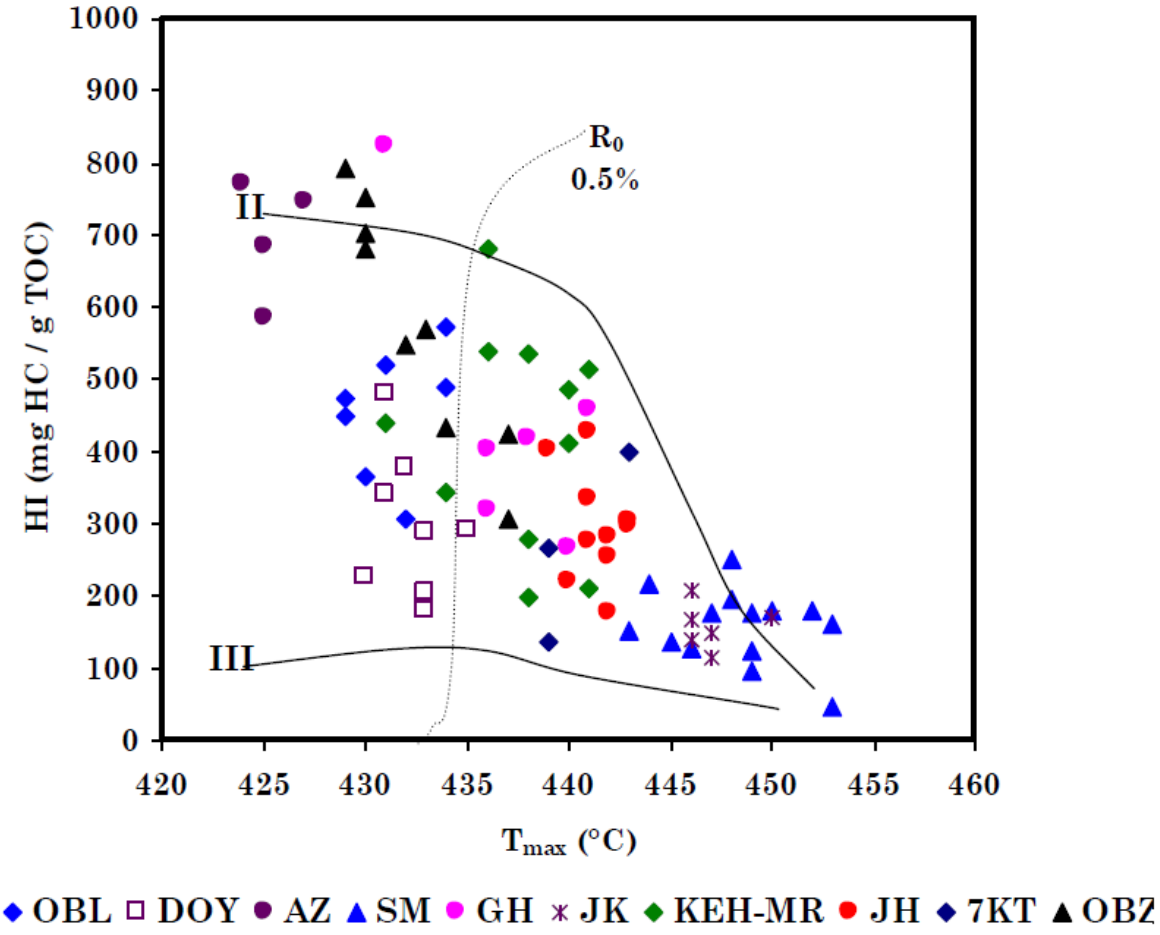
1000
900
800
700
600
500
400
300
200
100
0
HI (mg HC / g TOC)
420
425
430
435
440
445
450
455
460
Tmax (°C)
R0
0.5%
II
III
OBL
DOY
AZ
SM
GH
JK
KEH-MR
JH
7KT
OBZ

Figure 3

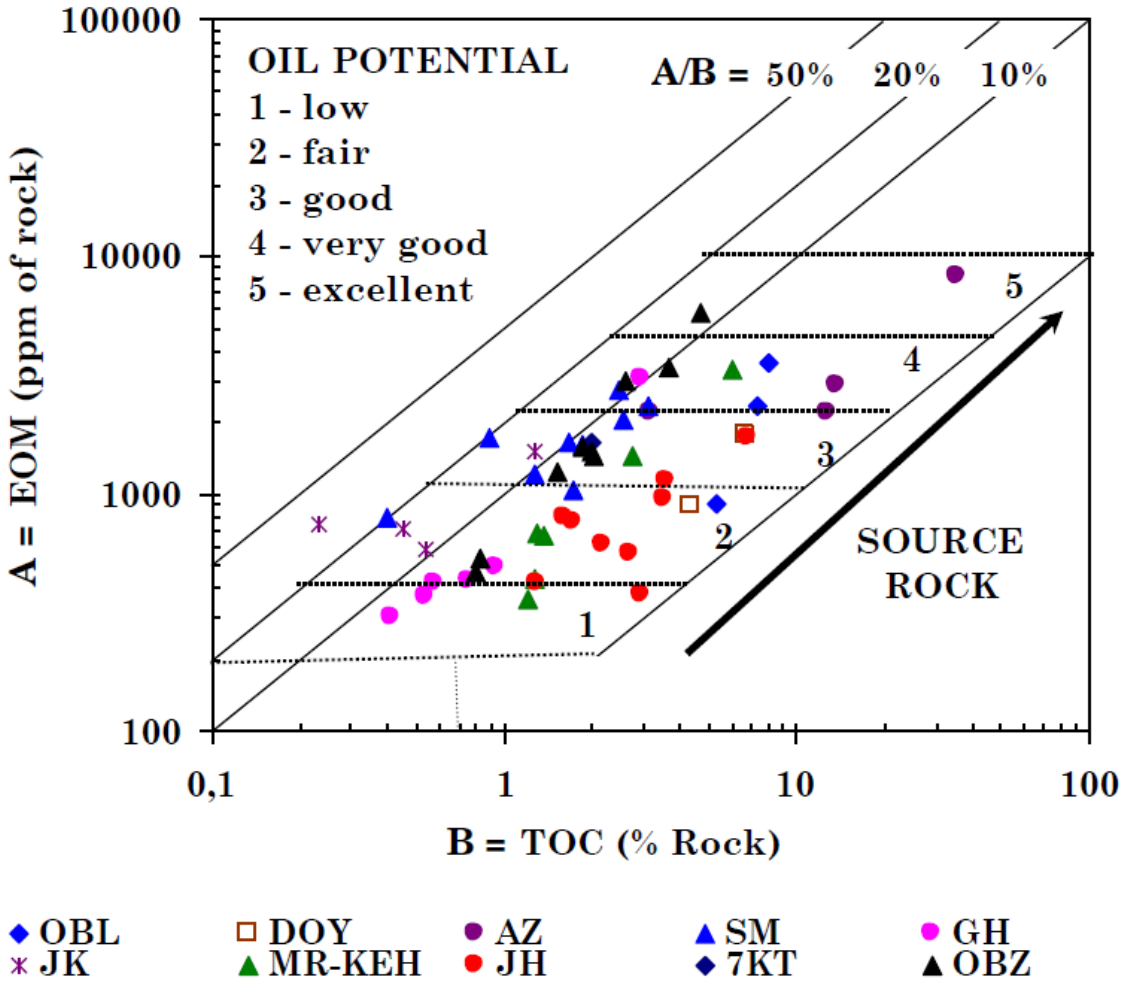
OIL POTENTIAL
1 - low
2 - fair
3 - good
4 - very good
5 - excellent
A/B = 50% 20% 10%
SOURCE ROCK
A = EOM (ppm of rock)
B = TOC (% Rock)
100000
10000
1000
100
0,1
1
10
100
OBL
JK
DOY
MR-KEH
AZ
JH
SM
7KT
GH
OBZ

Figure 4

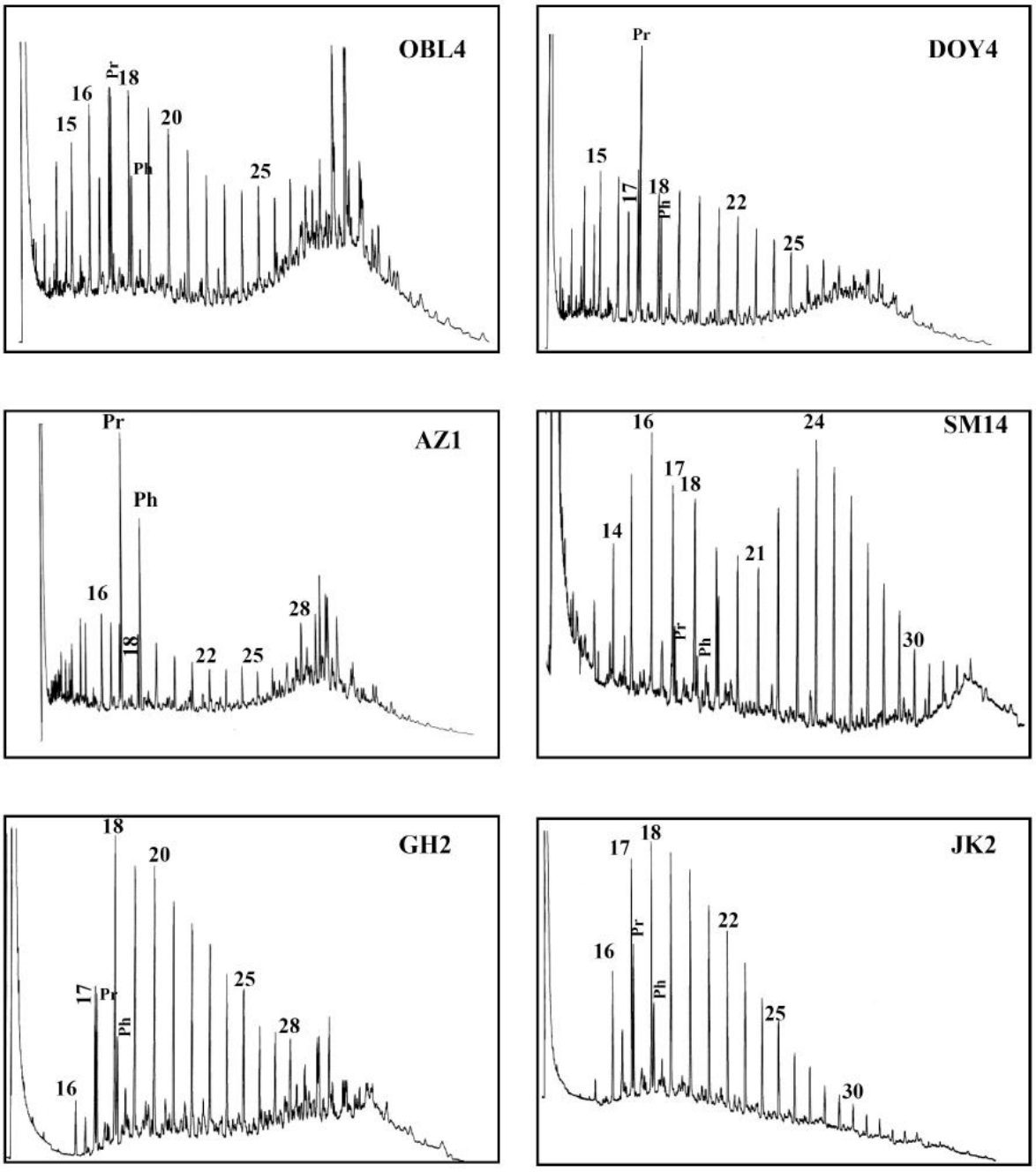
OBL4
15
16
Pr
18
20
Ph
25
DOY4
Pr
15
17
18
Ph
22
25
AZ1
Pr
Ph
16
18
22
25
28
SM14
16
24
17
18
14
21
Pr
Ph
30
GH2
18
20
17
Pr
Ph
25
28
16
JK2
17
18
16
Pr
22
Ph
25
30

Figure 4 continued

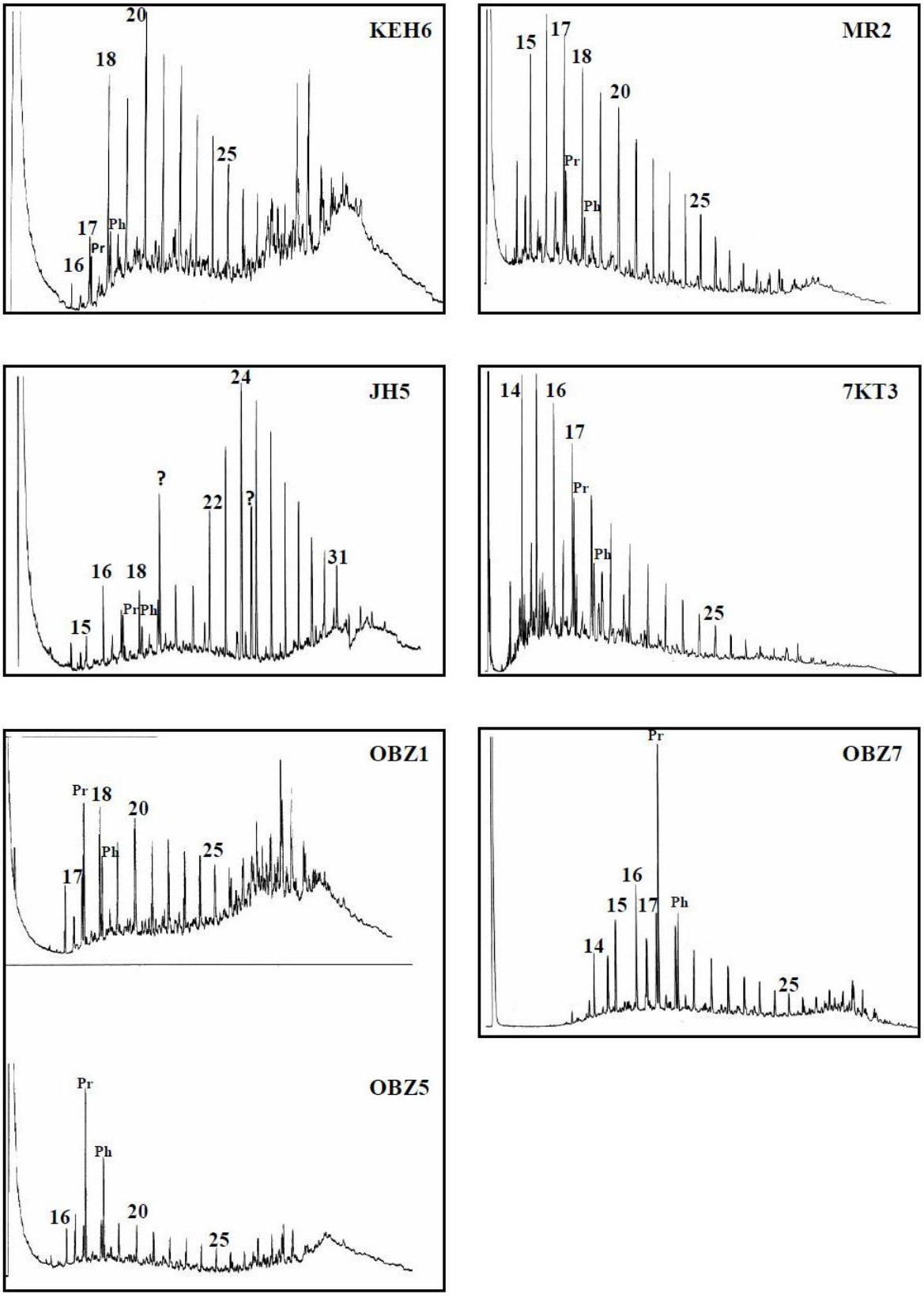

Figure 5

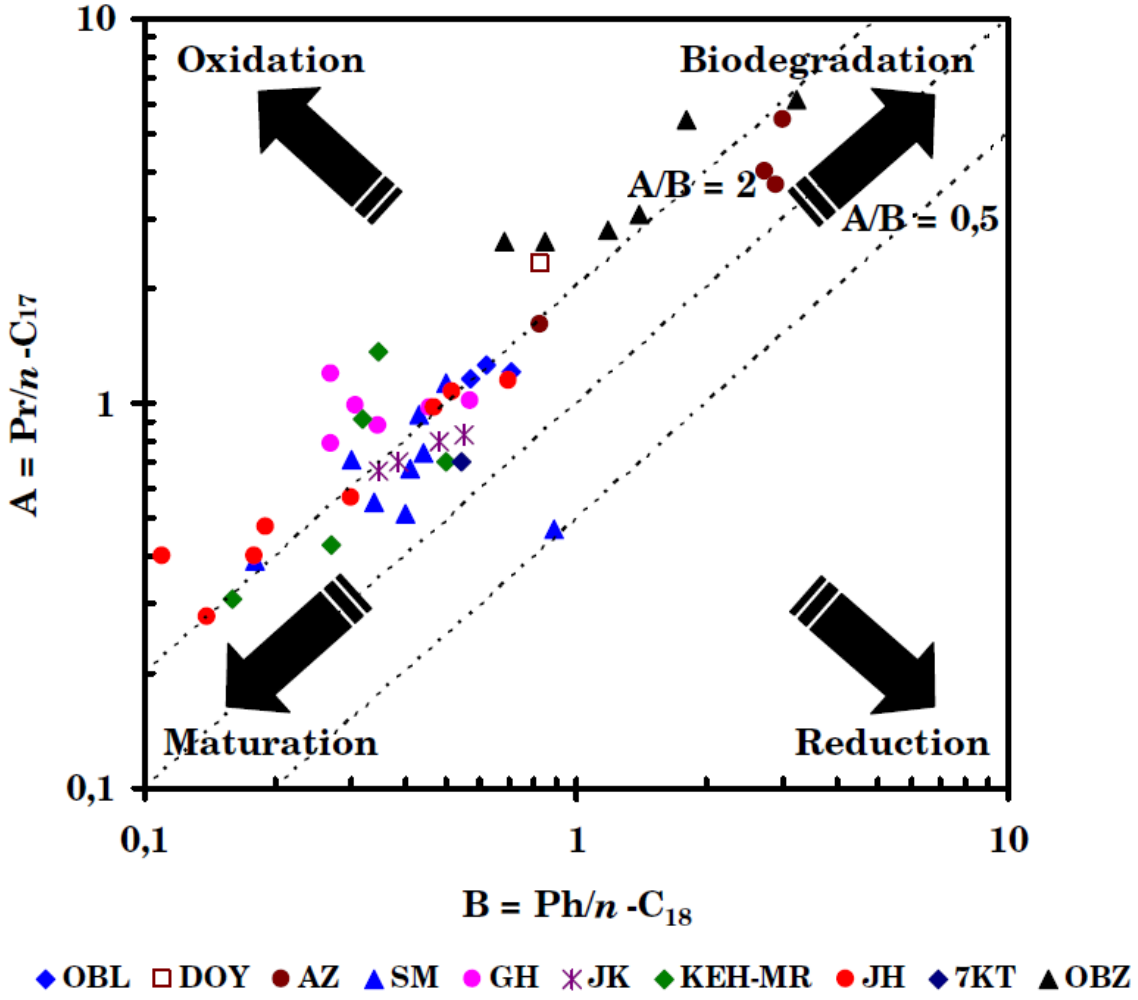
10
1
0,1
0,1
1
10
Oxidation
Biodegradation
A/B = 2
A/B = 0,5
Maturation
Reduction
A = Pr/n -C17
B = Ph/n -C18
OBL
DOY
AZ
SM
GH
JK
KEH-MR
JH
7KT
OBZ

Figure 6

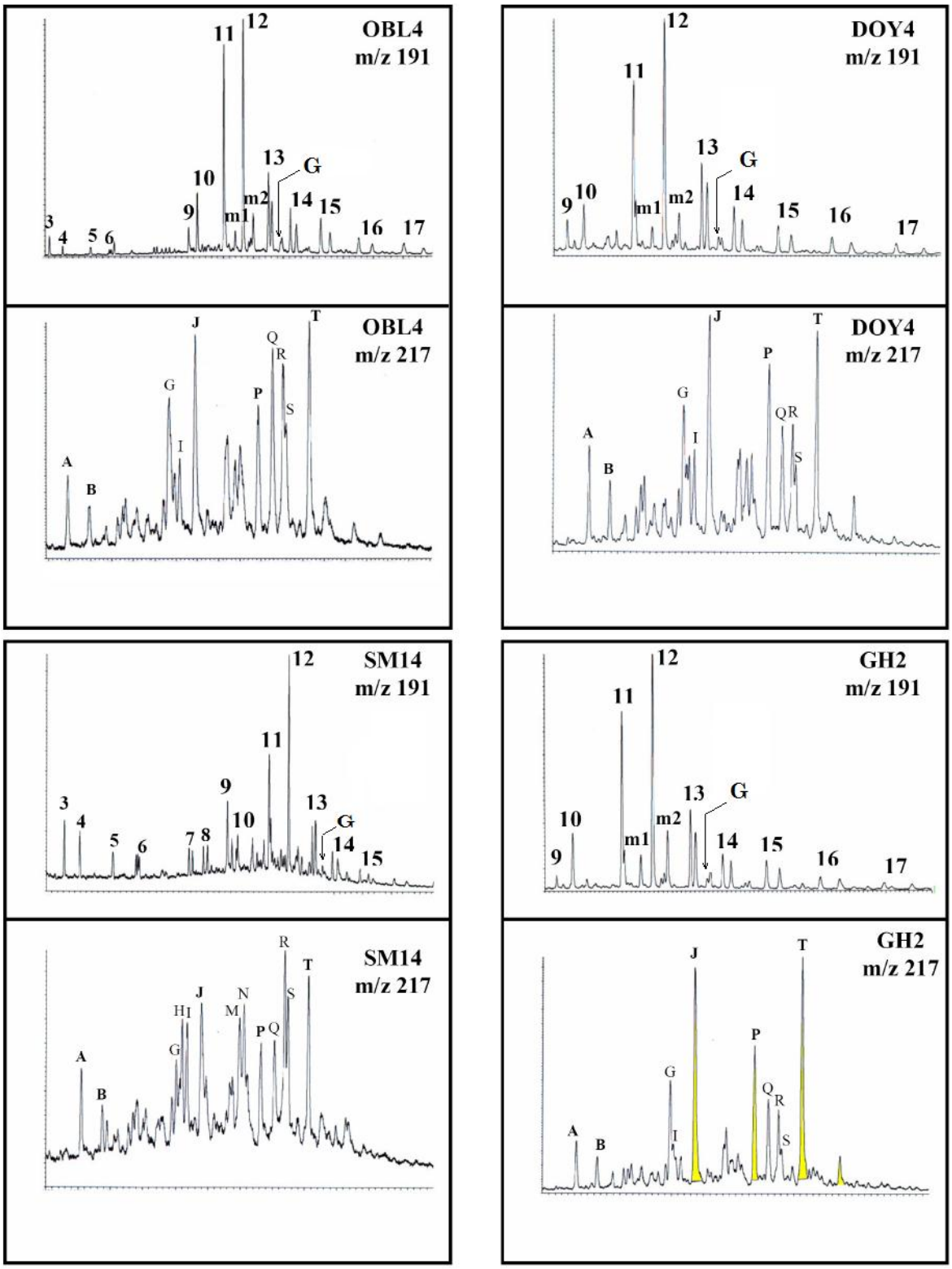
OBL4
m/z 191
3
4
5
6
9
10
11
12
m1
m2
13
G
14
15
16
17
OBL4
m/z 217
A
B
G
I
J
P
Q
R
S
T
DOY4
m/z 191
DOY4
m/z 217
SM14
m/z 191
SM14
m/z 217
GH2
m/z 191
GH2
m/z 217

Figure 6 continued

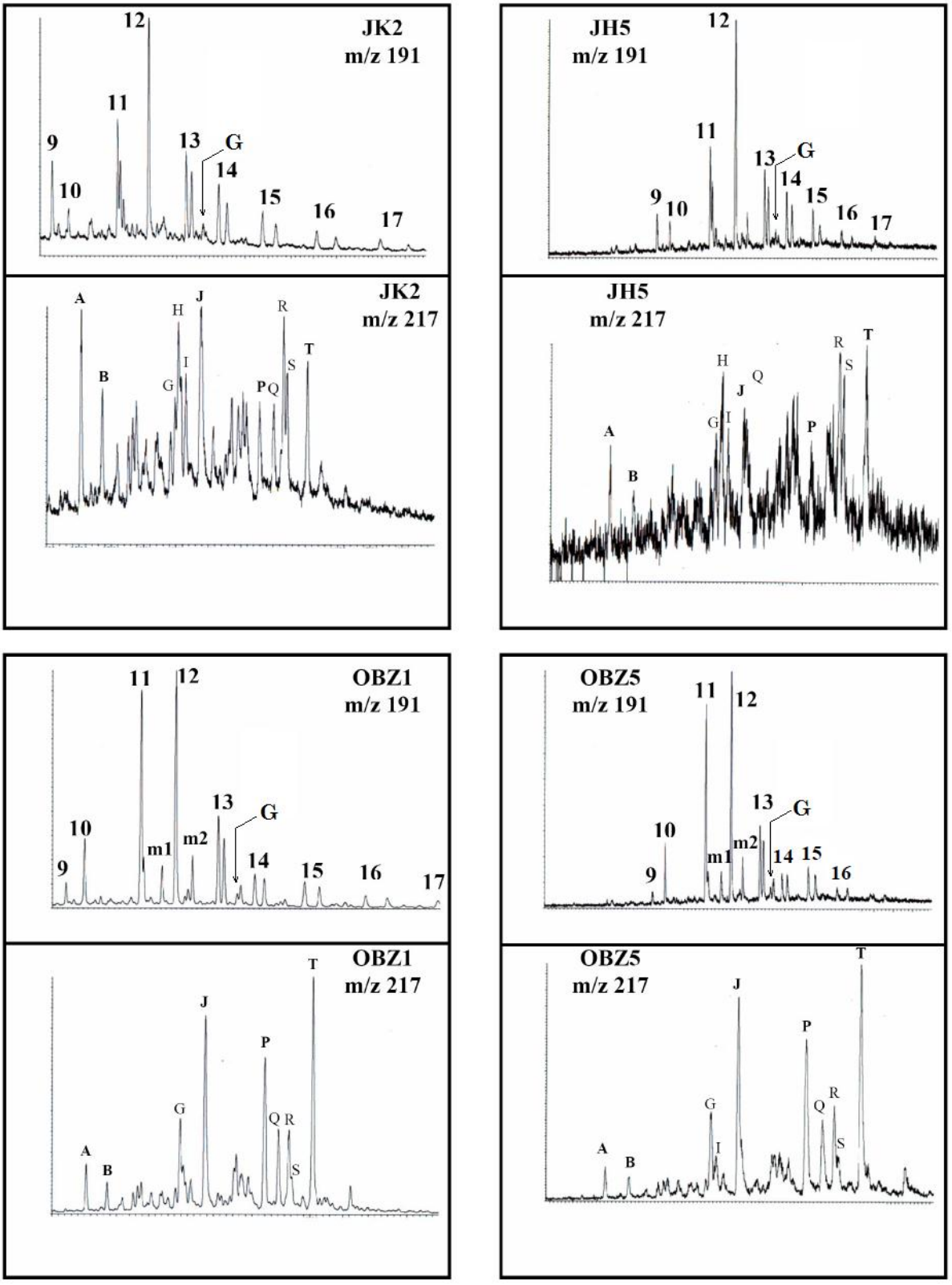

Figure 7

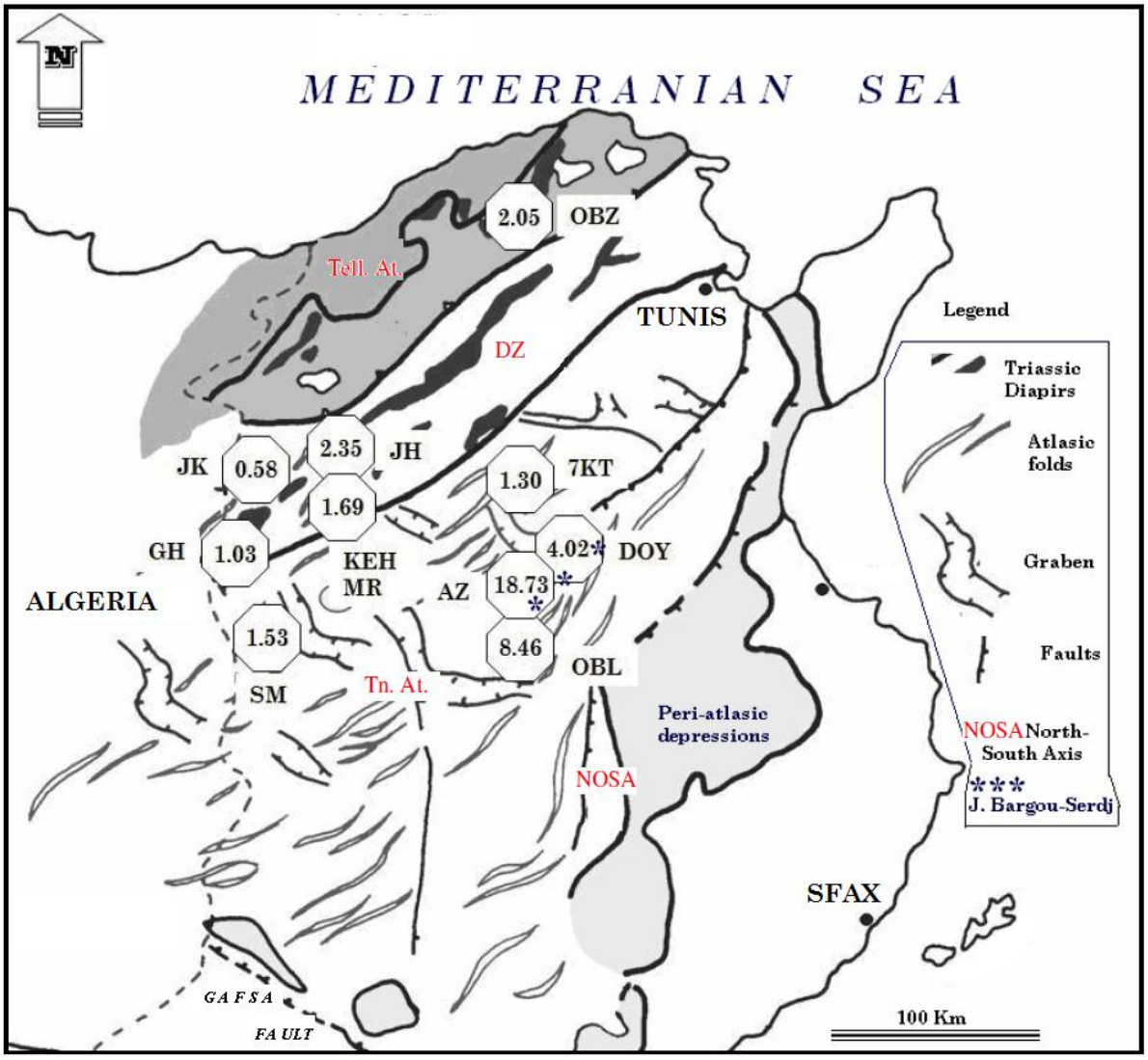
MEDITERRANIAN SEA
N
2.05
OBZ
Tell. At.
TUNIS
DZ
Legend
Triassic Diapirs
Atlasic folds
Graben
Faults
NOSA North-South Axis
J. Bargou-Serdj
JK
0.58
2.35
JH
1.69
1.30
7KT
GH
1.03
KEH
MR
4.02
DOY
AZ
18.73
ALGERIA
1.53
SM
8.46
OBL
Tn. At.
Peri-atlasic depressions
NOSA
SFAX
GAFSA
FAULT
100 Km

Figure 8

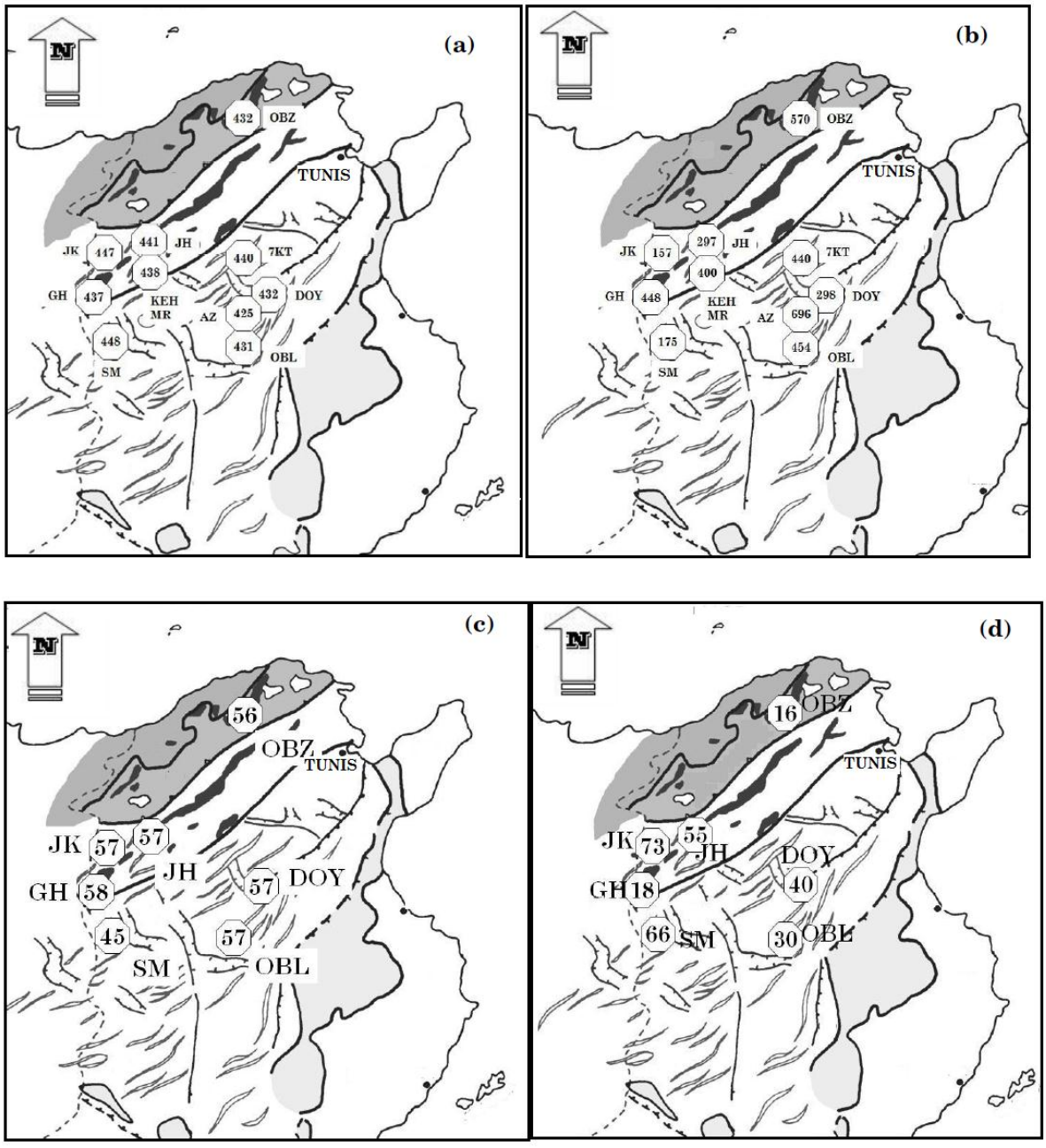
(a)
N
432
OBZ
TUNIS
JK
447
441
JH
438
440
7KT
GH
437
KEH
MR
AZ
425
432
DOY
448
431
OBL
SM
(b)
N
570
OBZ
TUNIS
JK
157
297
JH
400
440
7KT
GH
448
KEH
MR
AZ
696
298
DOY
175
454
OBL
SM
(c)
N
56
OBZ
TUNIS
JK
57
57
JH
GH
58
57
DOY
45
57
SM
OBL
(d)
N
16
OBZ
TUNIS
JK
73
55
JH
DOY
GH
18
40
66
SM
30
OBL

Figure 9

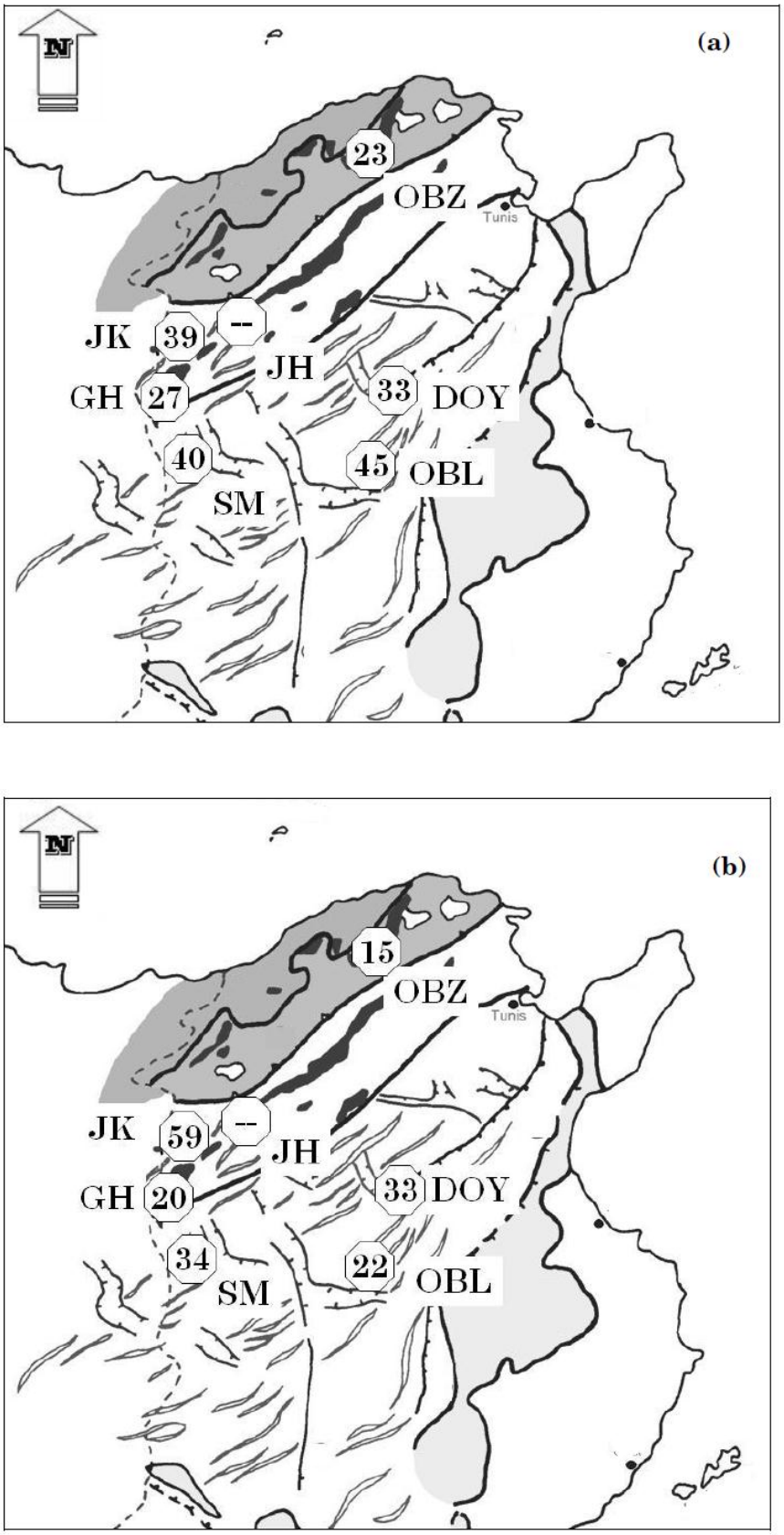
N
(a)
23
OBZ
Tunis
JK
39
--
JH
GH
27
33
DOY
40
45
OBL
SM
N
(b)
15
OBZ
Tunis
JK
59
--
JH
GH
20
33
DOY
34
22
OBL
SM

Figure 10

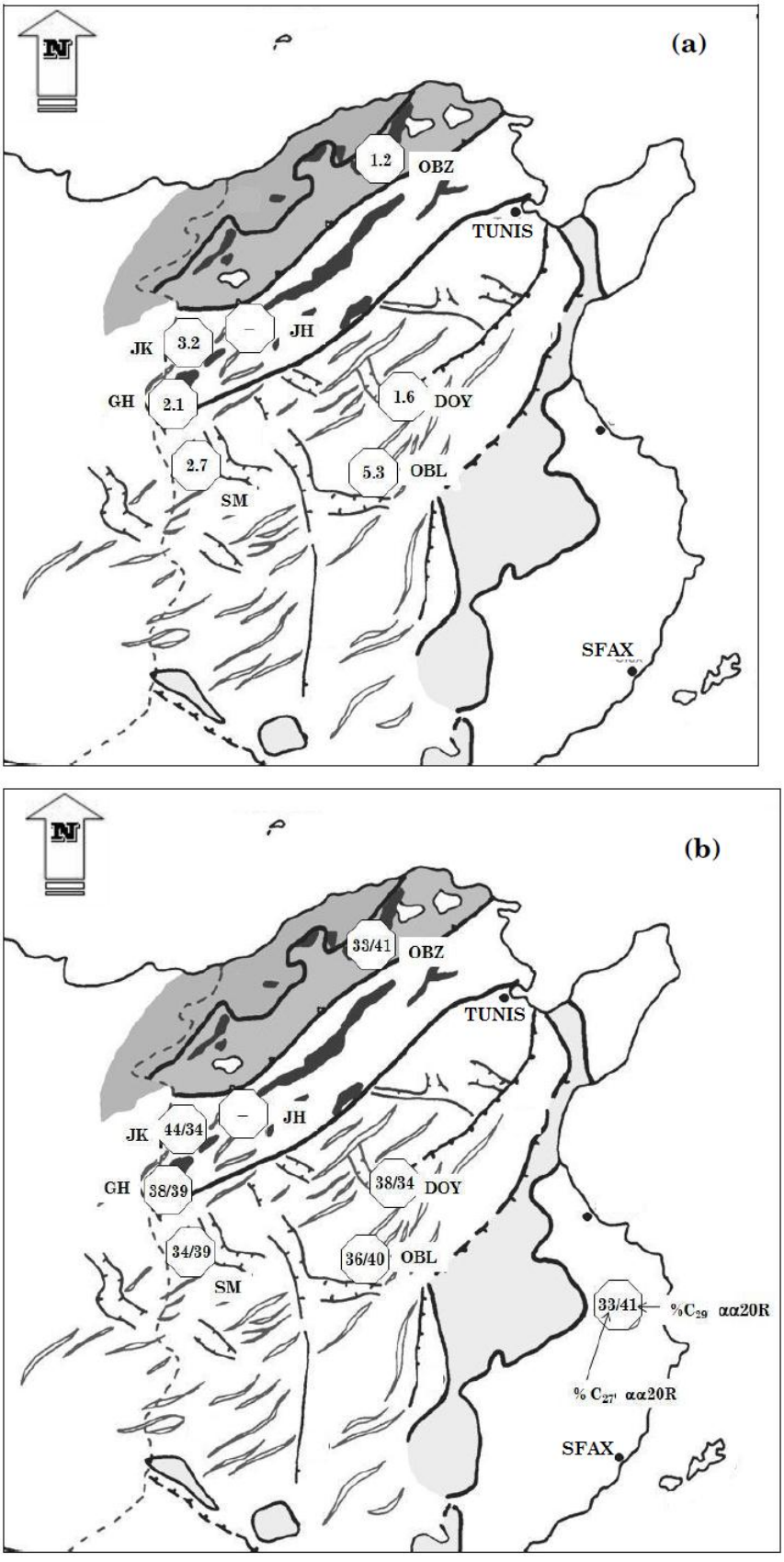
(a)
N
1.2
OBZ
TUNIS
JK
3.2
JH
GH
2.1
1.6
DOY
2.7
5.3
OBL
SM
SFAX
(b)
N
33/41
OBZ
TUNIS
JK
44/34
JH
GH
38/39
38/34
DOY
34/39
36/40
OBL
SM
33/41
%C29 αα20R
% C27 αα20R
SFAX

Table 1

Sample	Name	Locality	Age	TOC R-E II (% R)[a]	S1 (mgHC/ g R)[b]	S2 (mgHC/ g R)[c]	PP (mgHC/ g R)[d]	PI (x100)[e]	HI (mgHC/ g TOC)[f]	T_{max} (°C)[g]
1B	OBL1	Od Bahloul	C/T	7.99	5.16	39.11	44.27	12	489	434
2B	OBL2	Od Bahloul	C/T	11.79	8.66	67.62	76.62	11	573	434
3B	OBL3	Od Bahloul	C/T	11.17	5.15	58.19	63.34	08	521	431
4B	OBL4	Od Bahloul	C/T	5.29	1.59	16.27	17.86	09	307	432
5B	OBL5	Od Bahloul	C/T	7.28	3.88	34.57	38.45	11	475	429
6B	OBL6	Od Bahloul	C/T	7.84	2.43	35.25	37.68	06	450	429
7B	OBL7	Od Bahloul	C/T	7.83	3.69	28.52	32.21	11	364	430
8B	DOY1	Ouled Yahia	C/T	3.04	1.15	6.86	8.01	14	225	430
9B	DOY2	Ouled Yahia	C/T	3.76	0.91	10.93	11.84	08	290	435
10B	DOY3	Ouled Yahia	C/T	5.90	0.79	16.97	17.76	04	287	433
11B	DOY4	Ouled Yahia	C/T	6.74	2.29	32.35	34.64	07	480	431
12B	DOY5	Ouled Yahia	C/T	4.47	1.23	15.24	16.47	07	341	431
13B	DOY6	Ouled Yahia	C/T	2.11	0.39	3.81	4.20	09	180	433
14B	DOY7	Ouled Yahia	C/T	4.39	1.15	16.60	17.75	06	378	432
15B	DOY8	Ouled Yahia	C/T	1.72	0.38	3.52	3.90	10	204	433
16B	AZ1	Aine Zakkar	C/T	35.59	19	275	294	06	772	424
17B	AZ5	Aine Zakkar	C/T	13.84	3.44	103.2	106.64	03	745	427
18B	AZ6	Aine Zakkar	C/T	12.60	3.73	73.89	77.62	05	586	425
19B	AZ7	Aine Zakkar	C/T	12.88	3.41	88.01	91.42	04	683	425
20B	SM5	Kalaat Senan	C/T	0.88	0.76	1.55	2.31	33	176	447
21B	SM7	Kalaat Senan	C/T	1.26	0.36	1.75	2.11	12	218	444
22B	SM8	Kalaat Senan	C/T	3.08	1.62	6.03	7.65	21	196	448
23B	SM9	Kalaat Senan	C/T	0.61	0.20	1.08	1.28	16	177	449
24B	SM10	Kalaat Senan	C/T	2.48	1.03	4.44	5.47	19	179	452
25B	SM11	Kalaat Senan	C/T	1.72	0.64	2.35	2.99	21	137	445
26B	SM12	Kalaat Senan	C/T	1.84	0.89	3.33	4.22	21	181	450
27B	SM13	Kalaat Senan	C/T	1.66	0.65	2.66	3.31	20	160	453
28B	SM14	Kalaat Senan	C/T	2.56	1.12	6.47	7.59	15	252	448
29B	SM15	Kalaat Senan	C/T	0.40	0.30	0.51	0.81	37	128	446
30B	SM16	Kalaat Senan	C/T	0.39	0.21	0.48	0.69	31	123	449
31B	GH1	GarnHalfaya	C/T	0.54	0.08	1.43	01.51	06	265	440
32B	GH2	GarnHalfaya	C/T	0.58	0.10	2.34	02.44	04	403	436
33B	GH3	GarnHalfaya	C/T	0.93	0.17	4.26	04.43	04	458	441
34B	GH4	GarnHalfaya	C/T	0.75	0.14	3.14	03.28	04	419	438
35B	GH5	GarnHalfaya	C/T	2.95	1.10	24.32	25.42	04	824	431
36B	GH6	GarnHalfaya	C/T	0.41	0.05	1.31	01.36	04	319	436
37B	JK1	Jebel Ksikiss	C/T	0.38	0.21	0.57	0.78	27	150	447
38B	JK2	Jebel Ksikiss	C/T	0.64	0.05	0.73	0.78	06	114	447
39B	JK3	Jebel Ksikiss	C/T	0.54	0.32	0.90	1.22	26	166	446
40B	JK4	Jebel Ksikiss	C/T	0.23	0.31	0.39	0.70	44	170	450
41B	JK5	Jebel Ksikiss	C/T	0.45	0.34	0.62	0.96	35	138	446
42B	JK6	Jebel Ksikiss	C/T	1.26	1.01	2.61	3.62	28	207	446
43B	KEH1	K^{t} Hamra	C/T	6.01	1.35	40.97	42.32	03	682	436
44B	KEH2	K^{t} Hamra	C/T	0.34	0.03	00.72	00.75	04	211	441
45B	KEH3	K^{t} Hamra	C/T	1.29	0.23	06.91	07.14	03	536	438
46B	KEH4	K^{t} Hamra	C/T	1.36	0.20	05.59	05.79	03	411	440
47B	KEH5	K^{t} Hamra	C/T	2.72	0.70	14.64	15.34	05	538	436
48B	KEH6	K^{t} Hamra	C/T	1.26	0.24	06.48	06.72	03	514	441
49B	KEH7	K^{t} Hamra	C/T	1.20	0.12	05.85	05.97	02	487	440
50B	KEH8	K^{t} Hamra	C/T	nd	0.02	00.54	00.56	04	nd	444
51B	MR1	MgotiRassou	C/T	1.56	0.11	03.10	03.21	03	199	438
52B	MR2	MgotiRassou	C/T	3.20	0.63	14.07	14.70	04	439	431
53B	MR3	MgotiRassou	C/T	1.06	0.21	03.66	03.87	05	345	434
54B	MR4	MgotiRassou	C/T	0.63	0.13	01.75	01.88	07	278	438
55B	JH1	Jebel Hadida	C/T	0.70	0.16	01.24	01.40	11	177	442
56B	JH2	Jebel Hadida	C/T	1.59	0.34	04.02	04.36	08	253	442
57B	JH3	Jebel Hadida	C/T	6.79	0.40	20.58	20.98	02	303	443
58B	JH4	Jebel Hadida	C/T	1.29	0.08	00.83	00.91	09	64	444
59B	JH5	Jebel Hadida	C/T	1.72	0.18	04.76	04.94	04	276	441
60B	JH6	Jebel Hadida	C/T	2.70	0.28	09.02	09.30	03	334	441
61B	JH7	Jebel Hadida	C/T	3.61	0.65	15.46	16.11	04	428	441
62B	JH8	Jebel Hadida	C/T	3.52	0.59	14.15	14.74	04	402	439
63B	JH9	Jebel Hadida	C/T	2.96	0.23	08.93	09.16	03	302	443
64B	JH10	Jebel Hadida	C/T	2.18	0.34	06.13	06.47	05	281	442
65B	JH11	Jebel Hadida	C/T	1.81	0.41	05.37	05.78	07	297	443
66B	JH12	Jebel Hadida	C/T	0.56	0.38	01.23	01.61	24	220	440
67B	7KT2	7 Koudiat	C/T	1.18	0.03	1.61	1.64	02	136	439
68B	7KT3	7 Koudiat	C/T	2.00	0.85	7.99	8.84	10	400	443

Table 1 continued

69B	7KT4	7 Koudiat	C/T	0.72	0.38	1.92	2.30	17	266	439
70B	OBZ1	Od.Bazina	C/T	0.82	0.14	03.48	03.62	04	424	437
71B	OBZ2	Od Bazina	C/T	3.66	1.07	24.91	25.98	04	680	430
72B	OBZ3	Od Bazina	C/T	1.52	0.45	08.66	09.11	05	570	433
73B	OBZ4	Od.Bazina	C/T	4.70	2.42	37.21	39.63	06	792	429
74B	OBZ5	Od. Bazina	C/T	2.62	1.10	19.68	20.78	05	751	430
75B	OBZ6	Od. Bazina	C/T	1.84	0.70	12.91	13.61	05	702	430
76B	OBZ7	Od. Bazina	C/T	2.02	0.56	11.04	11.60	05	547	432
77B	OBZ8	Od. Bazina	C/T	1.90	0.48	09.52	10.00	05	501	429
78B	OBZ9	Od. Bazina	C/T	0.65	0.18	02.82	03.00	06	434	434
79B	OBZ10	Od. Bazina	C/T	0.80	0.80	02.45	03.25	25	306	437

[a] Total organic carbon (% rock); [b] free hydrocarbons (mg HC/g rock); [c] potential hydrocarbons (mg HC/g rock); [d] production potential, PP= S1+S2 (mg HC/g rock); [e] Production index, PI=S1/(S1+S2)x100 (%); [f] hydrogen index, HI=S2x100/T.O.C (mgHC/gT.O.C); [g] S2 maximum peak temperature (°C). Samples (1, 2, 3,…, etc) are selected from base to top of each section.

Table 2

Name	TOC (% R.) [a]	EOM (‰ R.) [b]	EOM (% TOC)	EOM Composition (%) NSO [c]	AHCs [e]	SHCs [d]	GC of SHCs Pr/Ph [f]	Pr/n-C17 [g]	Ph/n-C18 [h]
OBL1	7.99	3.54	04.4	49	40	11	2.06	1.21	0.71
OBL4	5.29	0.90	01.7	73	22	05	1.82	1.16	0.57
OBL5	7.28	2.33	03.2	57	36	07	1.92	1.25	0.62
DOY4	6.74	1.78	02.6	48	45	07	2.67	2.29	0.83
DOY7	4.39	0.88	02.0	83	09	08	Nd	Nd [i]	Nd
AZ1	35.6	8.18	02.3	18	62	20	1.37	4.01	2.74
AZ3	3.15	2.18	06.9	64	28	08	1.84	1.61	0.83
AZ5	13.84	2.87	02.1	68	24	08	2.27	5.45	3.01
AZ7	12.88	2.20	01.7	77	16	07	2.45	3.68	2.91
SM5	0.88	1.71	19.4	13	74	13	2.25	1.13	0.50
SM7	1.26	1.21	09.6	62	22	16	1.21	0.93	0.43
SM8	3.08	2.33	07.6	35	56	09	1.68	0.68	0.41
SM10	2.48	2.77	11.2	70	23	07	0.38	0.47	0.89
SM11	1.72	1.03	06.0	76	16	08	1.38	0.74	0.44
SM12	1.84	1.60	08.7	26	63	11	1.59	0.55	0.34
SM13	1.66	1.66	10.0	61	17	22	1.52	0.52	0.40
SM14	2.56	2.06	08.0	37	51	12	2.42	0.39	0.18
SM15	0.40	0.79	19.8	83	14	02	2.60	0.71	0.30
GH1	0.54	0.37	06.8	67	22	11	1.41	0.79	0.27
GH2	0.58	0.42	07.2	67	23	10	2.17	0.99	0.31
GH3	0.93	0.49	05.3	72	24	04	1.85	0.97	0.46
GH4	0.75	0.43	05.7	77	16	07	1.17	1.02	0.57
GH5	2.95	3.04	10.3	66	24	10	2.84	0.87	0.35
GH6	0.41	0.30	07.3	83	10	07	1.55	1.19	0.27
JK2	0.64	0.59	10.9	43	38	19	1.50	0.70	0.39
JK4	0.23	0.75	32.6	56	35	09	1.69	0.80	0.48
JK5	0.45	0.72	16.0	51	39	10	1.52	0.67	0.35
JK6	1.26	1.50	11.9	39	51	10	1.50	0.83	0.55
KEH1	6.01	3.32	05.5	71	16	13	Nd	Nd	Nd
KEH3	1.29	0.68	05.3	77	12	11	1.06	0.31	0.16
KEH4	1.36	0.66	04.8	68	25	07	Nd	Nd	Nd
KEH5	2.72	1.46	05.4	73	21	06	Nd	Nd	Nd
KEH6	1.26	0.44	03.5	70	23	07	1.13	0.91	0.32
KEH7	1.20	0.36	03.0	78	13	09	0.72	1.37	0.35
MR2	3.20	2.17	06.8	64	26	10	1.73	0.43	0.27
MR3	1.06	0.80	07.5	48	40	12	1.48	0.70	0.50
JH2	1.59	0.80	05.0	84	12	04	1.32	1.07	0.52
JH3	6.79	1.73	02.5	78	12	10	Nd	Nd	Nd
JH4	1.29	0.42	03.2	78	13	09	1.08	1.15	0.70
JH5	1.72	0.77	04.5	37	42	21	1.46	0.98	0.47
JH6	2.70	0.56	02.1	70	20	10	1.91	0.40	0.11
JH7	3.61	1.14	03.2	61	23	13	1.50	0.57	0.30
JH8	3.52	0.94	02.7	61	22	17	1.45	0.28	0.14
JH9	2.96	0.38	01.3	57	33	10	1.99	0.40	0.18
JH10	2.18	0.61	02.8	74	15	11	1.56	0.48	0.19
7KT3	2.00	1.64	08.2	56	34	10	1.61	0.70	0.54
OBZ1	0.82	0.54	06.6	58	23	19	1.50	2.62	0.68
OBZ2	3.66	3.44	09.4	64	15	21	Nd	Nd	Nd
OBZ3	1.52	1.23	08.1	54	26	20	0.65	5.46	1.80
OBZ4	4.70	5.28	11.2	45	40	15	Nd	Nd	Nd
OBZ5	2.62	2.97	08.8	36	40	24	1.60	6.20	3.25
OBZ6	1.84	1.59	08.6	39	42	19	3.11	2.82	1.18
OBZ7	2.02	1.44	07.1	60	30	10	2.22	3.11	1.40
OBZ8	1.90	1.50	07.5	42	39	19	3.09	2.65	0.85
OBZ10	0.80	0.47	05.9	47	32	11	Nd	Nd	Nd

[a] Total organic carbon; [b] chloroform extractable OM; [c] nitrogen, sulfur and oxygen heteroatomic compounds; [d] saturated hydrocarbons; [e] aromatic hydrocarbons; [f] pristane/phytane peak height ratio; [g] pristane/*n*-heptadecane peak height ratio; [h] phytane/*n*-octadecane peak height ratio; [i] not determined.

Table 3

Steranes **GC-MS *m/z* 217**	**Terpanes** **GC-MS *m/z* 191**
A – 13β(H), 17α(H)-20S C27 Diasterane B – 13β(H), 17α(H)-20R C27 Diasterane G - 13β(H),17α(H)-24-methyl diacholestane (20S) + 14α,17α-cholestane (20S) H - 13β,17α-24-ethyldiacholestane (20S) + 14β,17β-diacholestane (20R) I – 14β,14β-cholestane (20S) + 13α,17β-24-methyldiacholestane (20R) J – 14α(H), 17α(H)-20R C27 (αα20R C27) O – 14β(H), 17β(H)20S C28 (ββ20S C28) P - 14α(H), 17α(H)20R C28, (αα20R C28) Q - 14α(H), 17α(H)20S C29 (αα20S C29) R - 14β(H), 17β(H)20R C29 (ββ20R C29) S - 14β(H), 17β(H)20S C29 (αα20S C29) T - 14α(H), 17α(H)20R C29 (αα20R C29)	**3** –Tricyclic Terpane C23 (C23T) **4** –Tricyclic Terpane C24 (C24T) **5** –Tricyclic Terpane C25 (C25T) **T** –Tetracyclic Terpane C24 (C24TeT) **6** –Tricyclic Terpane C26 (C26T) **7** –Tricyclic Terpane C28 (C27T) **8** –Tricyclic Terpane C29 (C28T) **9** – 18α(H)-22,29,30-trisnorneohopane (Ts) **10** - 17α(H)-22,29,30-trisnorhopane (Tm) **11** – 17α(H), 21β(H)–norhopane (C29H) **m1** – 17β(H), 21α(H)–normoretane (C29M) **12** – 17α(H),21β(H)–hopane (C30H) **m2** – 17β(H), 21α(H)–moretane (C30M) **13** – 17α(H),21β(H)-C31 homohopane (22S + 22R) **G –** Gammacerane; pentacyclic terpane (C30H52) **14** – 17α(H),21β(H)-C32 bishomohopane (22S +22R) **15** – 17α(H),21β(H)-C33 trishomohopane (22S + 22R) **16** – 17α(H),21β(H)-C34 tetrakishomohopane (22S + 22R) **17** – 17α(H),21β(H)-C35 pentakishomohopane (22S + 22R)

Table 4

Sample	TT/TS [a]	%Ts [b]	29H/30H [c]	29M/30H [d]	30M/29M [e]	29M/29H [f]	30M/30H [g]	$\%SC_{31}$ [h]	$\%SC_{32}$ [i]	$\%SC_{33}$ [j]	23T/30H [k]
OBZ1	1.34	24	0.91	0.11	1.82	0.12	0.2	54	54	59	nd
OBZ5	1.20	16	0.85	0.13	1.46	0.15	0.19	56	52	56	nd
DOY4	1.59	40	0.73	0.09	1.77	0.12	0.16	57	59	62	0.11
OBL4	5.33	30	0.85	0.09	1.77	0.1	0.16	57	61	62	0.08
SM14	2.72	66	0.53	nd	nd	nd	nd	45	60	57	0.26
GH2	2.15	18	0.75	0.14	1.72	0.18	0.24	58	56	57	0.06
JK2	3.19	73	0.53	nd	nd	nd	nd	57	59	60	0.09
JH5	nd	55	0.44	nd	nd	nd	0.14	57	56	64	nd

Legend:

[a] TT/TS: Total Terpanes/Total Steranes ratio = [$\alpha\beta C_{29}$+$\alpha\beta C_{30}$] Hopane / [$\alpha\alpha$20R-C_{27}+ $\alpha\alpha$20R-C_{28}+ $\alpha\alpha$20R-C_{29}] Steranes

[b] %Ts = Ts x 100/Ts+Tm: 18α(H)22,29,30-Trisnorneohopane x 100/(18α(H)Trisnorneohopane + 17α(H)22,29,30-Trisnorhopane)

[c] 29H/30H: 17α(H),21β(H)norhopane/ 17α(H),21β(H)hopane

[d] 29M/30H: 17β(H),21α(H)normoretane/ 17α(H),21β(H)hopane

[e] 30M/29M: 17β(H),21α(H)moretane/ 17β(H),21α(H)normoretane

[f] 29M/29H: 17β(H),21α(H)normoretane/ 17α(H),21β(H)norhopane

[g] 30M/30H: 17β(H),21α(H)moretane/ 17α(H),21β(H)hopane

[h] $\%SC_{31}$: 17α(H),21β(H)22S-homohopane x 100/[17α(H),21β(H)22S-homohopane + 17α(H),21β(H)22R-homohopane]

[i] $\%SC_{32}$: 17α(H),21β(H)22S-bishomohopane x 100/[17α(H),21β(H)22S-bishomohopane + 17α(H),21β(H)22R-bishomohopane]

[j] $\%SC_{33}$: 17α(H),21β(H)22S-trishomohopane x 100/[17α(H),21β(H)22S-trishomohopane + 17α(H),21β(H)22R-trishomohopane]

[k] 23T/30H: C_{23}Tricyclic terpane/17α(H),21β(H)hopane

nd: not determined

Table 5

Samples	TT/TS [a]	%C_{27} [b]	%C_{28} [c]	%C_{29} [d]	C_{27}/C_{29} [e]	%ααS [f]	%ββR [g]	Dia. Index [h]	%SDia [i]
OBZ1	1.34	33	26	41	0.80	25	nd	20	62
OBZ5	1.2	35	26	39	0.90	23	nd	15	61
DOY4	1.59	38	28	34	1.12	33	34	33	62
OBL4	5.33	36	24	40	0.90	45	nd	22	74
SM14	2.72	34	27	39	0.87	40	52	34	66
GH2	2.15	38	23	39	0.97	27	nd	20	62
JK2	3.19	44	22	34	1.29	39	56	59	65
JH5	nd	nd	nd	nd	nd	nd	nd	nd	nd

Legend

[a] TT/TS: Total Terpanes/Total Steranes ratio = [αβC_{29}+αβC_{30}] Hopane / [αα20R-C_{27}+ αα20R-C_{28}+ αα20R-C_{29}] Steranes

[b] %C_{27}: αα20R-C_{27}Sterane x 100/ (αα20R-C_{27}+ αα20R-C_{28}+ αα20R-C_{29}) Steranes

[c] %C_{28}: αα20R-C_{28}Sterane x 100/ (αα20R-C_{27}+ αα20R-C_{28}+ αα20R-C_{29}) Steranes

[d] %C_{29}: αα20R-C_{29}Sterane x 100/ (αα20R-C_{27}+ αα20R-C_{28}+ αα20R-C_{29}) Steranes

[e] C_{27}/C_{29}: αα20R-C_{27} Sterane x 100/(αα20R-C_{29})Sterane

[f] %ααS: αα20S-C_{29} Sterane x 100 / [αα20R-C_{29} + αα20S-C_{29}] Sterane

[g] %ββR: ββ20R-C_{29} Sterane x 100 / [ββ20R-C_{29} + αα20R-C_{29}] Steranes

[h] Dia. Index: Diasterane Index = [13β(H),17α(H)20(S+R)-C_{27}Diasteranes]/ [13β(H),17α(H)20(S+R)-C_{27}Diasteranes + αα20(S+R)-C_{29}Sterane]

[i] %SDia: 13β(H),17α(H)20S-C_{27}Diasterane x 100/ [13β(H),17α(H)20S + 13β(H),17α(H)20R]-C_{27} Diasteranes

nd: not determined